

**A COMPARATIVE EROSIVE WEAR STUDY OF WELD OVERLAY ON
AS CAST 21-4-N AND 23-8-N STEELS**

A DISSERTATION

*Submitted in partial fulfillment of the
requirements for the award of the degree*

of

MASTER OF TECHNOLOGY

in

MECHANICAL ENGINEERING

(With Specialization in Welding Engineering)

By

NISHANT KAMBOJ



DEPARTMENT OF MECHANICAL AND INDUSTRIAL ENGINEERING

INDIAN INSTITUTE OF TECHNOLOGY ROORKEE

ROORKEE - 247667 (INDIA)

JUNE, 2019

CANDIDATE DECLARATION

I hereby declare that the work carried out in this dissertation entitled, “**A Comparative Erosive Wear Study of Weld Overlay on As Cast 21-4-N and 23-8-N Steels**”, is presented on behalf of partial fulfillment of the requirement for the award of the degree of “Masters of Technology” with specialization in “**Welding Engineering**”, submitted to the department of Mechanical and Industrial Engineering department, Indian Institute of Technology, Roorkee, under the supervision of **Dr. Navneet Arora** Professor, Mechanical and Industrial Engineering Department, Indian Institute of Technology, Roorkee, India.

I have not submitted the matter embodied in this Semester Report for award of any other degree.

Dated:

Place: Roorkee.

(NISHANT KAMBOJ)

CERTIFICATION

This is to certify that the above statement made by the candidate is correct to the best of my knowledge and belief.

Dr. NAVNEET ARORA

Professor, Mechanical and Industrial Engineering Dept.

ACKNOWLEDGEMENT

The euphoria and joy, accompanying the successful completion of my task would be incomplete without the special mention of the person whose guidance and encouragement made my effort successful.

I am deeply indebted to my guide **Dr. Navneet Arora**, Professor in the department of **Mechanical and Industrial Engineering, Indian Institute of Technology**, Roorkee, whose help, stimulating suggestions and encouragement helped me in my all time to make my effort successful.

I am also grateful to all faculty members and staff of MIED, Indian Institute of Technology, Roorkee.

I extend my thanks to all my friends who have helped directly or indirectly for the completion of this research proposal.

Finally, I would like to express my deepest gratitude to the Almighty for showering blessings on me. I gratefully acknowledge my heartiest thanks to all my family members for their inspirational impetus and moral support during the course of work.

Nishant Kamboj

Enrollment No.: 17542005

M.Tech-2nd year

ABSTRACT

The objective of the study was the examination of erosion wear rate of Nitronic steel welds using a slurry jet at high speed where impingement angle and time of particles attacking were controlled. Here the experiments were conducted on the apparatus which impinge high velocity jet of slurry of silica sand particles. The angle in this study was varied from 30 degree to 90 degree and time was varied from 30 min to 90 min. The examined samples include base metal (21-4-N steel and 23-8-N)) as well as two types of gas metal arc welded samples by ER2209 filler metal with argon as shielding gas. The erosive wear study was conducted by silica sand particles of size varying from 100 μm to 500 μm . The results of the study were plotted as the calculated mass loss of eroded samples versus the angle of impingement and time of erosion.

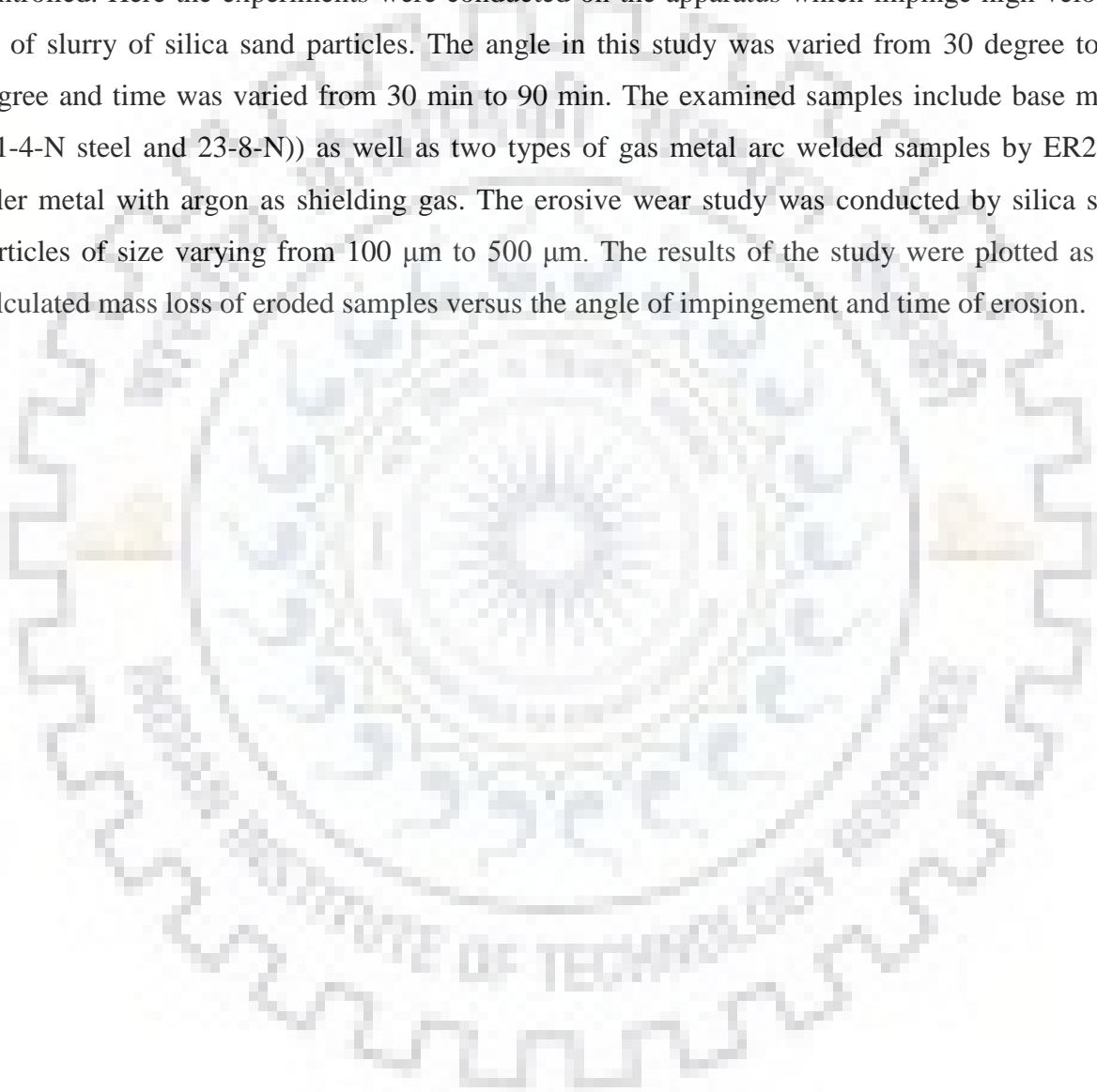


TABLE OF CONTENTS

	Acknowledgement	I
	Abstract	II
	Contents	III
	List of Figures	VII
	List of Tables	IX
	Nomenclature	X
	CHAPTER 1	
	INTRODUCTION	1
1.1	APPLICATIONS OF HIGH NITROGEN STEELS	1
1.2	WEAR	2
1.3	TYPES OF WEAR	2
1.3.1	Abrasive Wear	2
1.3.2	Adhesive Wear	2
1.3.3	Erosive Wear	3

1.3.4	Corrosive Wear	3
1.3.5	Fatigue Wear	3
1.4	EROSION WEAR	3
1.5	MECHANISM OF EROSION WEAR	4
1.5.1	Cutting Mechanism	4
1.5.2	Ploughing Mechanism	5
1.5.3	Subsurface Deformation and Cracking	6
1.6	PARAMETERS AFFECTING EROSION WEAR	6
1.6.1	Impact angle	6
1.6.2	Velocity of solid particles	6
1.6.3	Hardness	6
1.6.4	Particle size and shape	7
1.6.5	Solid concentration	7
1.7	THESIS STATEMENT	7
	CHAPTER 2	
	LITERATURE SERVEY	8

	CHAPTER 3	
	PROBLEM FORMULATION	21
	CHAPTER 4	22
	EQUIPMENT, MATERIALS, EXPERIMENTAL PROCEDURES	22
4.1	BASE MATERIAL PROPERTIES	22
4.1.1	Chemical Composition	22
4.2	WELDING	23
4.2.1	Welding Process	23
4.2.2	Welding Parameters	25
4.2.3	Filler Metals	25
4.3	HARDNESS TESTING	26
4.4	EROSIVE WEAR STUDY	27
4.5	FE-SEM	30

	CHAPTER 5	
	RESULTS AND DISCUSSIONS	31
5.1	MICROSTRUCTURAL EXAMINATION	31
5.2	HARDNESS TESTING	33
5.3	EFFECT OF TIME ON EROSIVE WEAR RATES	36
5.4	FE-SEM ANALYSIS	39
	CHAPTER 6	
	CONCLUSION	43
6.1	FUTURE SCOPE	44
	REFERENCES	45

LIST OF FIGURES

Fig. 1.1: Cutting Mechanisms	5
Fig. 1.2: Ploughing Mechanism	5
Fig. 2.1: Micrograph of (a) 13/4 martensitic stainless steel and (b) 21/4-N nitronic steel	8
Fig. 2.2: Graph between cumulative weight versus erosion time at impact angles of (a) 30° and (b) 90°	9
Fig. 2.3: Curve for ductile materials erosion rate developed by Finnie	10
Fig. 2.4: Curve for brittle materials erosion rate developed by Finnie	11
Fig. 2.5: Curve for jet slurry erosion developed by Levi	12
Fig. 4.1: Nitronic steel (21-4-N and 23-8-N steel)	22
Fig. 4.2: GMAW welding	24
Fig. 4.3: Welded sample	24
Fig. 4.4: Hardness testing setup	26
Fig. 4.5: (a) Front view (b) Side view (c) Close view of Jet-Type Slurry erosion test machine	28
Fig. 4.6: Sample orientation	29
Fig. 4.7: Samples after Erosion testing (a) 21-4-N and (b) 23-8-N	30
Fig. 4.8: FE-SEM machine	30
Fig. 5.1: 21-4-N (a) Optical micrograph of base metal, (b) Optical micrograph of As weld, and (c) Optical micrograph of weld with quench	31
Fig. 5.2: 23-8-N (a) Optical micrograph of base metal, (b) Optical micrograph of As weld, and (c) Optical micrograph of weld with quench	32
Fig. 5.3: Hardness profiles of 21-4-N base metal, As weld and weld with quench as a function of distance (mm) (plotted on x-axis).	33
Fig. 5.4: Hardness profiles of 23-8-N base metal, As weld and weld with quench as a function of distance (mm) (plotted on x-axis).	34
Fig. 5.5: Hardness profiles of 21-4-N (a) base metal, (b) As weld and (c) weld with quench as a function of distance (mm) (plotted on x-axis) before and after test	35
Fig. 5.6: Hardness profiles of 23-8-N (a) base metal, (b) As weld and (c) weld with quench as a function of distance (mm) (plotted on x-axis) before and after test	35
Fig. 5.7: Variation in cumulative weight loss with respect to time at 30° impact angle (23-8-N)	36

Fig. 5.8: Variation in cumulative weight loss with respect to time at 60° impact angle (23-8-N)	37
Fig. 5.9: Variation in cumulative weight loss with respect to time at 90° impact angle (23-8-N)	37
Fig. 5.10: Variation in cumulative weight loss with respect to time at 30° impact angle (21-4-N)	38
Fig. 5.11: Variation in cumulative weight loss with respect to time at 60° impact angle (21-4-N)	38
Fig. 5.12: Variation in cumulative weight loss with respect to time at 90° impact angle (21-4-N)	38
Fig. 5.13: Base metal (21-4-N) (a) 30 degree, (b) 60 degree, and (c) 90 degree	39
Fig. 5.14: As weld (21-4-N) (a) 30 degree, (b) 60 degree, and (c) 90 degree	40
Fig. 5.15: Weld with quench (21-4-N) (a) 30 degree, (b) 60 degree, and (c) 90 degree	40
Fig. 5.16: Base metal (23-8-N) (a) 30 degree, (b) 60 degree, and (c) 90 degree	41
Fig. 5.17: As weld (23-8-N) (a) 30 degree, (b) 60 degree, and (c) 90 degree	41
Fig. 5.18: Weld with quench (23-8-N) (a) 30 degree, (b) 60 degree, and (c) 90 degree	42

LIST OF TABLES

Table 4.1: Chemical composition of the 21-4-N Nitronic steel (wt.%)	22
Table 4.2: Chemical composition of the 23-8-N Nitronic steel (wt.%)	23
Table 4.3: Welding number as per filler and shielding gas used	23
Table 4.4: Optimum Welding Parameters	25
Table 4.5: Chemical composition of filler metal	25
Table 4.6: Mechanical properties of filler metal	26
Table 4.7: Erosion Parameters	29



NOMENCLATURE

GMAW	Gas Metal Arc Welding
SMAW	Shielded Metal Arc Welding
kV	Kilo Volt
AISI	American Irons and Steels Institute
HP	Horse Power
FE-SEM	Field Emission Scanning Electron Microscope
UTS	Ultimate Tensile Strength
YS	Yield Strength



Chapter 1

INTRODUCTION

Due to increasing demand of alternative sources of electric energy production, the hydro power plants are being made in rivers where silt content is high thus blades used in Hydro turbines for electric energy production is subjected to serious situations that make erosion to the blades of turbine. Materials of these items are chosen to help oppose erosion and drag out their financial life. A standout amongst the most widely recognized materials in the manufacture of hydro turbine blades is 304L stainless steel which is having good erosion resistance properties. The research is being done to get the alternative material which is having more erosion resistance than existing material. One of the materials is High nitrogen steels.

High-quality austenitic stainless steels can be created by supplanting carbon with nitrogen. The solid-solubility of nitrogen is more than carbon, is an intense interstitial solid-solution strengthener, solid austenite stabilizer, and enhances resistance to corrosion due to pitting. Despite the fact that in liquid iron the solvency of nitrogen is low, 0.045 wt.% at 1600 °C at atm. pressure, through alloying and concentrated high-pressure dissolving techniques [1], the nitrogen levels which can be acquired is over 1 wt.% and An austenitic stainless steel ought to be viewed as "high-nitrogen" on the off chance that it contains the amount of nitrogen more than that can be present in material by preparing at atm. Pressure, for most of the alloys and this limiting point is around 0.4 wt.%.

1.1. APPLICATIONS OF HIGH NITROGEN STEELS

- Bearings in aviation turbines, Ball screw gearing shafts which move airplane's flap traces.
- Rams in water cooled turbo drills and screws, Fasteners for the chemical, car.
- Water supply and control structures, Sewage treatment plant structures, mining equipment – magnetic ore separator screens, Bulk solids handling equipment – conveyor parts and many other applications.
- Naval, Pumps, valves and fittings, Fasteners, cables, chains, Screens and wire cloth, Marine hardware, boat, Pump shafting, Heat exchanger part.

1.2. WEAR

Wear is the loss of material from a portion in view of a mechanical relationship with another object. Many sorts of solids, liquids, and even gasses at high speed can evacuate material and change the physical measurement and usefulness of a segment. Corrosion and erosion are the essential drivers of wear. Corrosion is achieved by concoction response of material with its encompassing. Erosion wear is a direct result of presentation to moving liquids and gasses, which could contain hard particulate. Effect of erosion wear in hydro turbines is pervasive increasingly when stood out from the corrosion. The administration life of hardware of slurry transport system is decreased by erosion brought on by strong liquid mix moving through the slurry transport structure. So slurry erosion is basic field should be investigated.

1.3. TYPES OF WEAR

There are several types and mechanisms of wear. These are: -

- 1.3.1. Abrasive wear
- 1.3.2. Adhesive wear
- 1.3.3. Erosion wear
- 1.3.4. Corrosive wear
- 1.3.5. Fatigue Wear

1.3.1. Abrasive Wear:

Abrasive wear can be characterized as the sort of wear that happens when a hard surface slides or contuse to have relative movement with a milder surface. Hard materials or asperity that cut groves amid this movement produces abrasive wear. These asperities can be those present in the tangling surface or any remote material. This generation of wear sections hurries the procedure of wear if not evacuated.

1.3.2. Adhesive Wear:

Adhesive wear can be characterized as the sort of wear that happens because of localized bonding between the reaching and the mating surfaces. In this sort of wear there is real exchange of material between the mating surfaces. This exchange relies on the level of hardness of the two

mating surface. Be that as it may, the precondition for this sort of wear is the intimate contact between the two surfaces. However, the use of greasing up surface, oil or grease diminishes the inclination of this sort of wear.

1.3.3. Erosive Wear:

This kind of wear is described as method of metal evacuation in view of impingement of strong particles on a surface. This can in like manner happen in light of gas and liquid however the erosion by this medium doesn't pass on.

1.3.4. Corrosive Wear:

Most metals are thermodynamically unsteady in environment and respond with oxygen to form oxides. These oxides form layer or scales over the surface. These scales are inexact attached to the surface.

1.3.5. Fatigue Wear:

Fracture Wear or break emerges when the segments are subjected to cyclic tension and compression over a limit stress. The surface wears out in this procedure. Vibration is the regular reason for fatigue.

1.4. EROSION WEAR

Erosion wear is a procedure of dynamic expulsion of material from an objective surface because of rehashed effects of solid particles. The particles suspended in the stream of strong fluid blend erode the targeting surface constraining the administration life of hydraulic turbines. Erosion wear brought on by the dynamic energy exchanged to target surface by impinging solid particles. Material loss of target material is higher for impinging molecule which is having higher kinetic energy. So speed at which particle impact has great influences on the Erosion wear of target material. Likewise, Erosion wear relies on upon the angle at which erodent strikes at target surface (effect edge), slurry focus, erodent measure, erodent shape and so on, the degree of Erosion wear changes material to material of target surface.

Erosion wear can be characterized into three classes:

1. Solid particle Erosion,
2. Slurry jet Erosion and
3. Cavitation Erosion.

Solid particle erosion is defined as the material volume loss when impingement of solid particles occurs on target material in the streaming liquid. The keep on striking of fluid stream on material surface causes slurry jet erosion. The disfigurement and expulsion of material from target surface because of rehashed nucleation, development and ballistic fall of air pockets is known as cavitation.

1.5. MECHANISM OF EROSION WEAR

Identifying the parameters which are affecting the erosion rates it is important to understand the mechanism by the removal of material occurs in erosion wear. Erosion wear is affected by following parameters:

1. Erodent material,
2. Impact speed,
3. Impact angle,
4. Target material,
5. Erodent size and shape, and
6. Carrier liquid.

The mechanism of erosive wear in ductile and brittle material is different. The mechanism of erosion wear includes ploughing, cutting and subsurface deformation and cracking.

1.5.1. Cutting Mechanism

When soft material is cut by hard material then the cutting wear is said to be occurred. So when the target material is impacted by impacting particle at positive rake angle and new surface is formed due to the cutting of chips from the material. The impinging particles shape in cutting wear is the main factor. The impinging particles having angular shape claims higher erosion wear due to cutting, because these impinging particles have sharp edges which act as cutting tool.

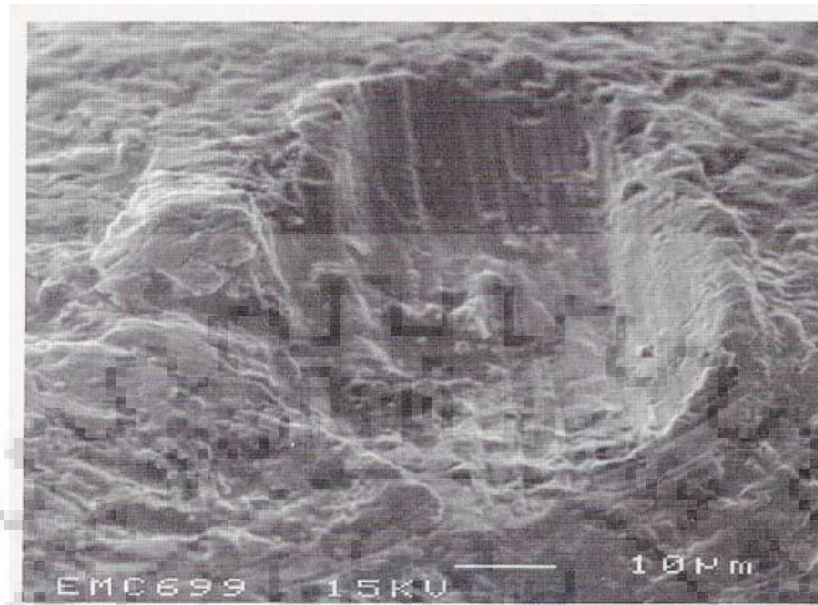


Fig. 1.1: Cutting Mechanisms [2]

1.5.2. Ploughing Mechanism

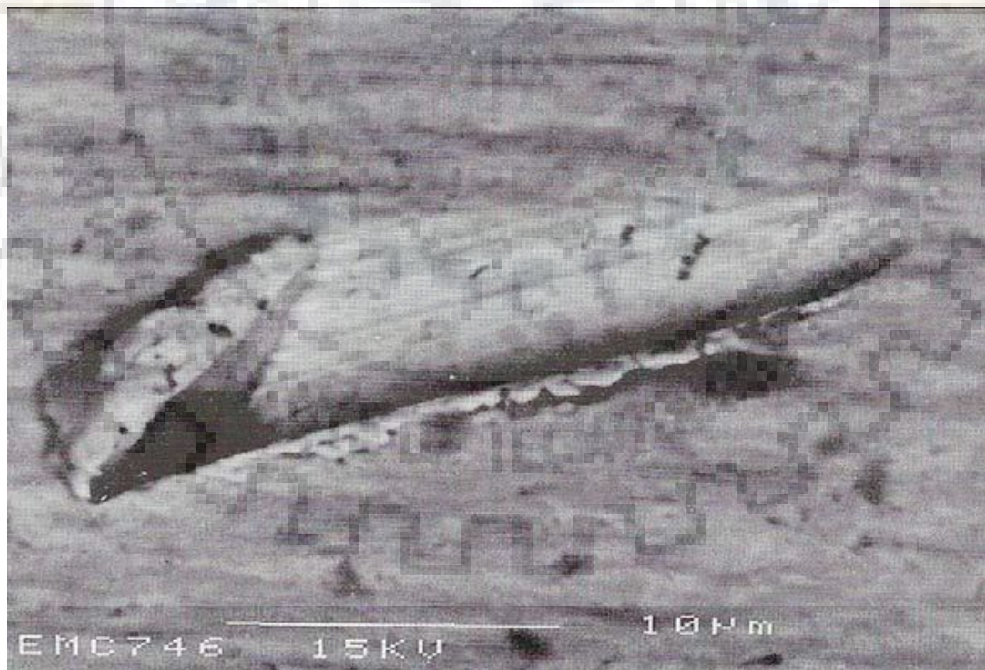


Fig. 1.2: Ploughing Mechanism [2]

Ploughing wear occurs when target material is strike by the particles of spherical shape at bigger negative rake angle which in the front of particles and the side of crater results in the raises lips due to displacing and shearing the target material. This lip is framed toward movement of erodent molecule or more a specific basic speed the lip gets removed from targeted surface. Compared to other mechanism this wear announced very less wear.

1.5.3. Subsurface Deformation and Cracking

When the target material is impacted by spherical particles then the plastic deformation takes place at that point due to high velocity of impacting particles. This plastic deformation brings about cracks and crater arrangement which spread and brittle fracture leads to wear. Expelled shear lip is shaped due to molecule impact. The shear lip severed by weariness created by rehashed effect of particles.

1.6. PARAMETERS AFFECTING EROSION WEAR

The parameters affecting erosion are as follows:

1.6.1. Impact angle

Impact angle can be termed as the angle between the surface targeted and the direction of velocity of the jet slurry. The erosion wear varies with impact angle on the basis of the mechanical properties of the target material such as either ductile or brittle material.

1.6.2. Velocity of solid particles

Erosive wear is strongly affected by the velocity of solid particles. Erosive wear strongly increases as the velocity of slurry increases. The relationship between the erosive wear rate and the velocity of slurry can be correlated by using power law according to which the velocity power index varies in the range of 2-4.

1.6.3. Hardness

Hardness can be defined as the property of the material by which it resists to permanent deformation. Erosive wear has been profoundly affected by the hardness of the material.

Hardness ratio can be characterized as the ratio of hardness of the material targeted and the hardness of the solid particles of the slurry.

1.6.4. Particle size and shape

Molecule shape and size is additionally the noticeable parameter, by which erosion wear is influenced. The size of solid particles has been considered important to erosion by many investigators. The power law determines the effect of increment in size of solid particle to the increment of erosive wear. The impact of molecule shape on the erosion is not set up because of challenges in characterizing the distinctive shape highlights. For the most part roundness calculation is taken thought. In the event that roundness component is one then the particles are impeccably circles and lower values demonstrate the molecule precision.

1.6.5. Solid concentration

Concentration is measure of strong particles by weight or by volume in the liquid. As convergence of molecule expands more particles strike the surface of impeller which increment the erosion rate, the concentration of slurries can shift from 2% to 50% on the sort of slurry. Be that as it may, at high concentration molecule cooperation increments and these abatements the striking speed of molecule at first glance.

1.7. THESIS STATEMENT

The objective of this study is to experimentally determine the relative slurry rates of two different types of nitronic steel (21-4-N and 23-8-N). The functional relationships among the rate of erosion, angle of particle impingement and time of erosion are established. Graphical representations are provided that compare the rate for the two weld conditions plus base metal in terms of angle of slurry flow and time of erosion.

Chapter 2

LITERATURE SURVEY

Chauhan et al. [3] has performed the experiment between 21-4-N nitronic steel and 13-4 martensitic steel to know the erosion behavior of hydro turbine steel by using slurry erosion jet machine. In both 30° and 90° , the 21/4-N nitronic steel gives a low erosion rate than 13/4 martensitic steel due to its high hardness value, high tensile toughness and microstructure present stabilized austenite phase with carbide. Variation in erosion graph is because at 30° impact angle, the surface degradation is due to shear cutting whereas in 90° impact angle, the damage of erosion is due to embrittlement and strain hardening of material.

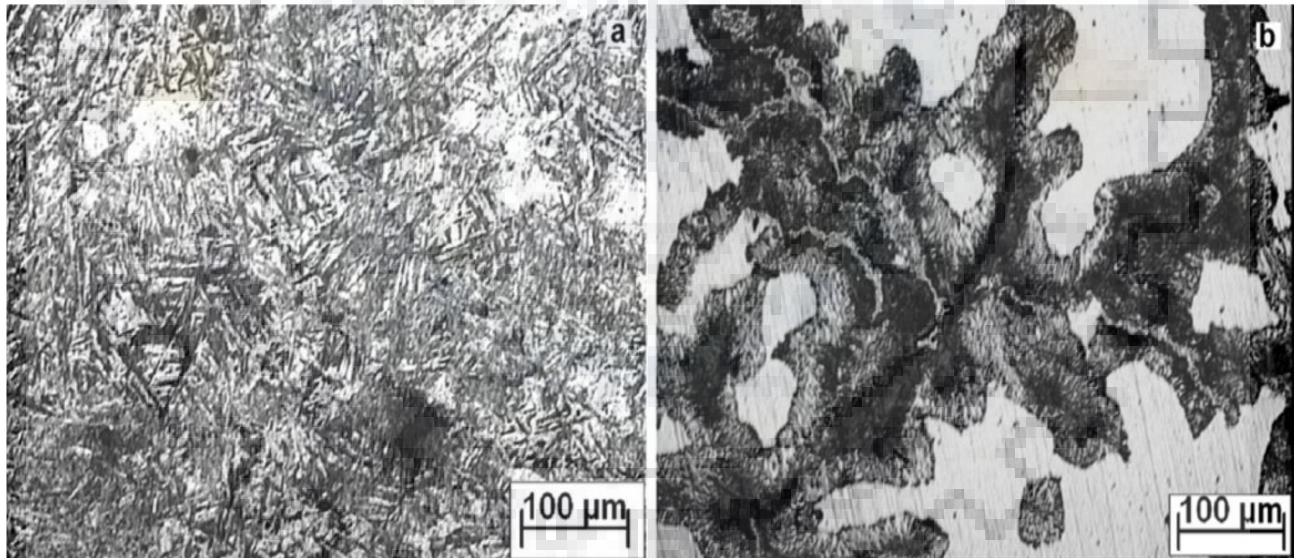


Fig. 2.1: Micrograph of (a) 13/4 martensitic stainless steel and (b) 21/4-N nitronic steel [3]

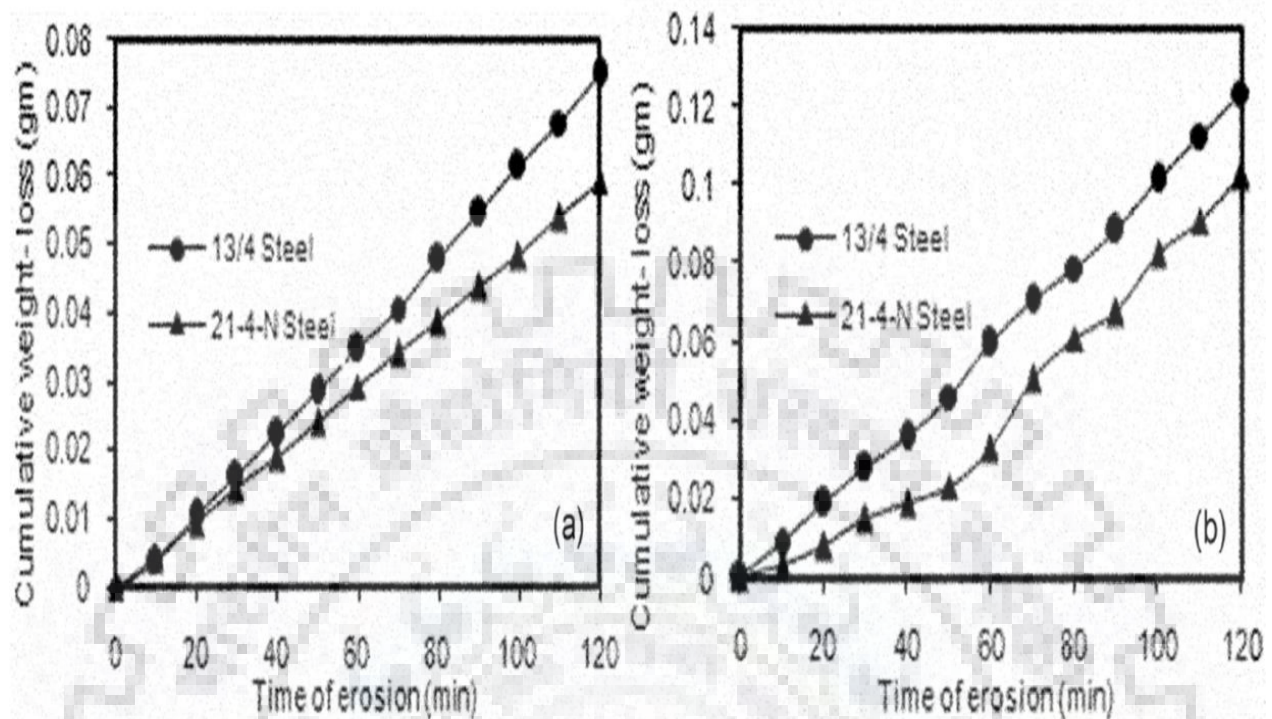


Fig. 2.2: Graph between cumulative weight versus erosion time at impact angles of (a) 30° and (b) 90° [3]

Santa et al. [4] concentrated the slurry and cavitation erosion resistance of six warm shower coatings in research center and contrasted with that of an uncoated martensitic stainless steel.

Shivamurthy et al. [5] has directed trials to concentrate the slurry erosive wear systems of Co-based Stellite and Ni-construct Colmonoy coatings in light of 13Cr-4Ni steels connected by Laser surface alloying (LSA) strategy. They perform analyze for a steady slurry speed of 12 m/s, for a settled slurry centralization of 10 kg/m³ sharp-edged SiO₂ particles with normal sizes of 375 and 100 μm and at impingement edges of 30°, 45°, 60°, and 90°. They pointed that when coatings affected with slurry particles of a normal size of 375 μm then stellite covering demonstrated flexible conduct while fragile if there should be an occurrence of colmonoy. Just a weak conduct was seen in both covering when affected with slurry particles of a normal size of 100 μm. They found that the disintegration rate diminishes in the coatings and the disintegration rate if there should be an occurrence of Ni-based steel is less when contrasted with Co-based covered steels.

Finnie [6] His exploration was led utilizing air to impel little strong particles through a tube at target surfaces and measure the subsequent mass loss. Finnie's research depended on the fact that the individual strong particles made a cut in the objective material when they came into contact. The subsequent cut in the objective material was illustrative of the amount of the cross area of every molecule infiltrated into the objective surface. Finnie built up bends to speak to the normal erosion rates for both malleable and brittle materials. The bends show the significance of the impingement angle on the subsequent erosion rate. In ductile erosion, the erosion rate achieves a top at around eighteen degrees and after that loses productivity as the angle winds up plainly more extreme. In the brittle erosion bend the erosion rate increments as the impingement angle increments. This would compare with the expanded effect vitality brought on by the normal impact.

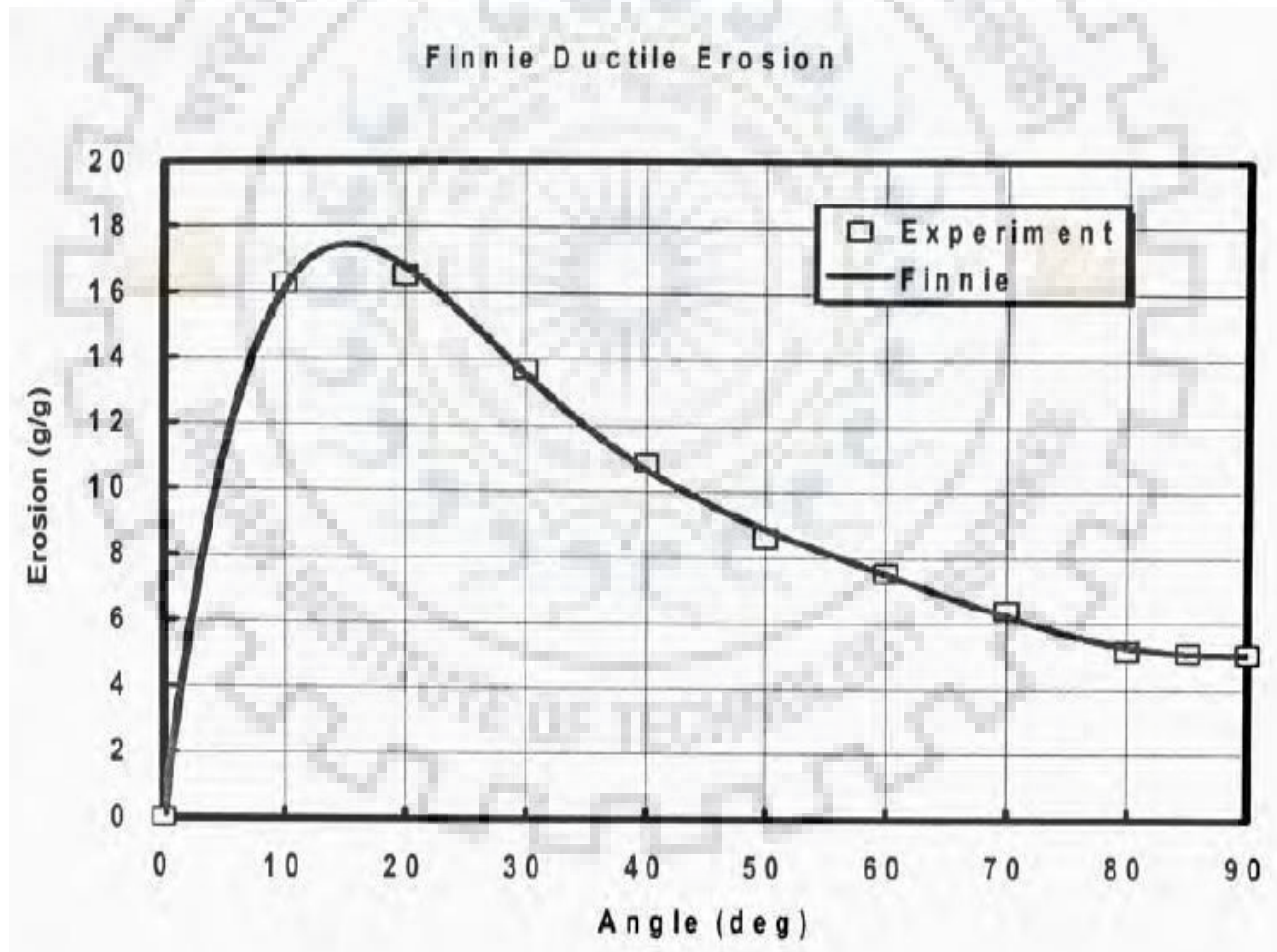


Fig. 2.3: Curve for ductile materials erosion rate developed by Finnie [6]

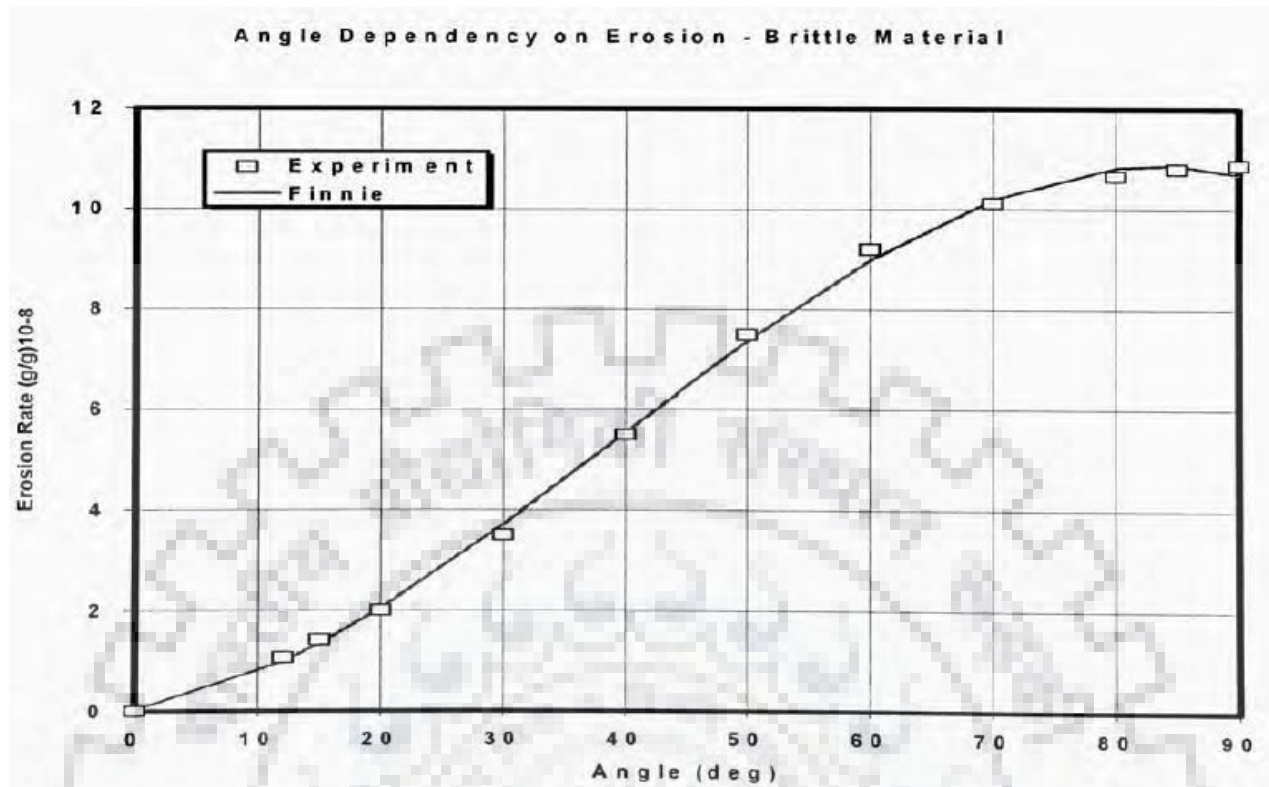


Fig. 2.4: Curve for brittle materials erosion rate developed by Finnie [6]

Levy [7] broadened the established erosion look into by including the investigation of erosion particles scattered in slurry. Slurry erosion is erosion that happens when particles entrained in a liquid make erosive wear a base material. Figure 2.4 is an average bend that Levy got tentatively for a flexible metal that was dissolved by slurry. This bend shape is fascinating a direct result of the bimodal way of the bend with a nearby least at around 60° and the neighborhood most extreme at 42°. In this bend, the erosion rate achieves a greatest at 90° like the brittle erosion bend. The moderate pinnacle speaks to the particles capacity to infiltrate the limit film that is made by the liquid. Collect watched this middle of the road crest in coal/lamp oil slurries and water/SiO slurries at low speed. Slurry erosion testing machines accessible are:

- Slurry pot erosion tester
- Slurry jet impingement.

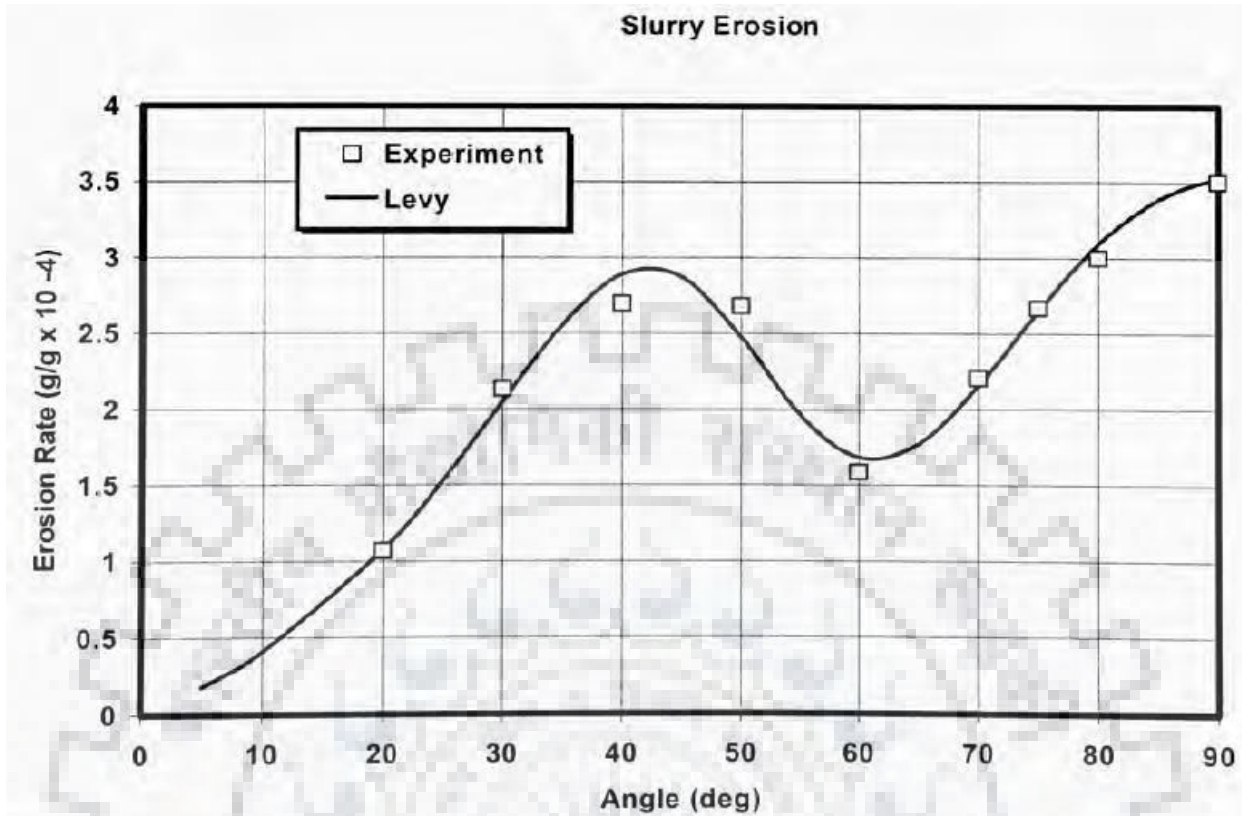


Fig. 2.5: Curve for jet slurry erosion developed by Levy [7]

Lin et al. [8] has conducted the test for finding the best welding process for welding high nitrogen steels for thickness of about 12 mm and founded that the best parameters for welding the high nitrogen steels with MIG welding were 260 ampere current with welding speed of 600 mm/min. torch height taken was about 15mm and angle of the torch was taken as 6°.

Mohammed et al. [9] conducted experiment of different welding process on welding of nickel free high nitrogen steel with four different welding process which were electron beam welding, SMAW, GTAW and friction stir welding. discontinuous ferrite network was found with electron beam welding in austenitic matrix, fully austenitic dendritic structure was found in SMAW, reverted austenitic pool were found in the weld zone in the martensitic matrix in GTAW weld, fine recrystallized austenitic grain structure was observed in nugget zone of the friction stir welds. Improved mechanical properties were found in the friction stir weld as compared to the other three welds. GTAW weld had the moderate strength lower than electron beam weld and friction stir weld.

O'Flynn et al. [10] assessed the erosion wear utilizing strong particles in He gas of Wc-17Co and $Cr_3C_2 + 25NiCr$ coatings on steel composite utilizing Sic as erodent. They assessed that covering helps in diminishing the erosion wear. At a point of 90° Wc-17Co demonstrates the better outcome however a low effect edges $Cr_3C_2 + 25NiCr$ was better.

Zu et al. [11] Designs a stream slurry erosion test fix. Utilizing this test fix they tried rectangular examples of aluminum, copper, mellow steel (containing 0.15% C) and alumina. The extent of examples was $35mm \times 30mm$ with thickness 3-5mm. They watched the connection between erosion rate and effect speed for 600 - 1000 μm silica sand slurry impinging onto aluminum. It was found that the material mass misfortune increment with expanding sway speed as per influence law, having a type $\delta (\log E/\delta (\log v)) = 2.7$. They watched that the erosion of alumina (a weak material), increments monotonically with impact angle, demonstrating a most extreme at close typical rate. The erosion rate of alternate metals conversely increments with expanding sway angle just a little angle of occurrence, with pinnacle erosion at around 40° , and gradually decrease at bigger effect points. All materials were tried at different parameters as slurry focus (0-30%), affect speed (0 to 8 m/s), and affect point (0° to 90°) and time. They watched that among all the four materials alumina demonstrate the most minimal erosion rate, and aluminum the most elevated. They found that the biggest contrast between the erosion resistance of alumina and other outstanding materials happens at a genuinely little impact angle of close to 30° - 40° , where the metals all have their most extreme erosion rates. The erosion resistance of alumina reduces as the impact angle increments towards 90° . Among every one of the four materials aluminum indicate most extreme wear rate then copper taken after by gentle steel and alumina demonstrate least wear rate. They found that the mass misfortune increment with increment in erosion as straight line albeit some ebb and flow toward a higher erosion time is after around 900 min. the erosion rate rise marginally over the initial 200 min then stay consistent up to a period around 900min and a moderate decrease is then watched, this last decay because of corruption of the erodent particles. The underlying ascent in erosion rate (to 200 min) is because of the moderate ascent in temperature seen amid the early running of the hardware. The most extreme decay is come to after around 2300 min.

Prasad et al. [12] has concentrated the slurry wear conduct of zinc-aluminum (Zn-59.8%, Al 37.5%, Cu-2.5%, Mg-0.2%) composites with and without the expansion of silicon substance by the

example revolution strategy over a scope of traversal speeds and separations. The amalgam for directing the tests were readied by means of the fluid metallurgy course as 20 mm measurement, 150 mm long barrel shaped castings. Solid metal molds were utilized for setting the compound gets soften in the required shape and size. The entire analyses were directed in a test fix. An electric engine was utilized to pivot the specimens in slurry over a scope of traversal separations (15 to 500 km) and paces (4.71 and 7.02 m/s). The slurry included 40% sand (212 to 300mm) particles suspended in an electrolyte (arranged by blending 5 cc concentrated sulphuric acid corrosive and 4gm sodium chloride in 10 L of water). In his outcomes he called attention to that wear rate of the examples expanded with separation before all else, achieved most extreme, and after that diminished from there on at longer traversal separations and wear increments with expanding the traversal speed independent of the compound synthesis. He additionally discovered that option of silicon enhanced the wear resistance (opposite of wear rate) of the composite framework.

Stack et al. [13] concentrated the consolidated impacts of slurry molecule focus and speed on the erosion–corrosion of a WC/Co–Cr covering in an engineered seawater arrangement containing sand particles and contrasted with the execution of a mellow steel presented to comparative conditions. They utilized examples of size 20mm×10mm×3mm having thickness of the covering fluctuated in the scope of 8–13 μm and 0.196 cm² range presented to impingement slurry stream. They set the test tests at a settled effect point of 90° to the impinging plane and a test directed for 30 min. The seawater slurry made out of silica sand with molecule estimate in the range 50–250 μm and focus differed at three qualities 4%, 6% and 8% (by mass %), and at two effect speeds to be specific 2 and 4 m/s.

Iwai et al. [14] has coordinated a Micro-Slurry-stream Erosion (MSE) test to rapidly evaluate the wear properties of thin single layered and multi layered coatings kept on built up carbide. Slurry containing 1.2μm alumina particles (hardness from 1800 to 2000 HV) was influenced at rapid (around 100 m/s) inverse to CVD TiC (TiN over TiC) and TiC coatings. The test piece was a square of 12.8mm with 5mm in height. In the event that there ought to be an event of CVD TiC/TiN covering they watched that wear significance of the TiN layer extended straightly until the point when the TiC layer was accomplished, where after it at first extended persevering at a low slant however kept an eye on increase in the midst of the area of the covering/substrate interface. They

assume that wear protection of the TiC layer was around two times higher than that of the TiN layer. The examination shows that wear rates were consistent inside the TiN and TiC layers, however demonstrated gigantic changes near the interfaces, especially that between the covering layer and the substrate. They watched that the wear rate of the TiC layer for the TiC/TiN covering almost relates with that of the single layered TiC, and was about bit of that of the TiN layer. They exhibited that TiC layer have around two times higher wear protection than the TiN layer.

Borse and Gandhi [15] had led trials to decide the ostensible size of multi-sized slurry speaking to the erosion wear and the impact of nearness of fine particles ($< 75\mu\text{m}$) in the slurry. Wear examples of dim cast iron were taken. The scope of introduction edge was 0° to 90° . The slurry was set up of water with sand gathered from the banks of stream Narmada. General particular gravity of sand was 2.68 and the last static settled fixation was seen as 53.7%. Mean molecule size of slurry was taken as $505\mu\text{m}$. The range for limited size particulate slurry was $112.5\mu\text{m}$ to $855\mu\text{m}$ and multi measured slurry was set up by blending parallel measure of various thin estimated slurries. In view of the consequences of their tests they presumed that for tight size slurry mean molecule size can be taken as the viable molecule measure though for multi estimated slurries, weighted mass molecule estimate is by all accounts better. It has likewise been inferred that impact of better particles in both thin and multi estimated slurries decreases the erosion wear.

Manisekaran et al. [16] had concentrated the effect of atom size and impingement on surface changed 13Cr-4Ni stainless steels (as they are overall used for hydro turbines also, water pumps). Trial of estimation of $50\times 50\text{ mm}^2$ were machined from 6 mm thick cast 13Cr-4Ni steel plates and the surface changes were done by two procedures particularly laser setting and beat plasma nitriding. Tests were finished in a test device to think the disintegration execution of balanced layers with two unmistakable erodent particle measure ranges (under 150 and 150-300 μm) in a silica sand slurry for 2 h at 90° . After surface transform they watched that beat plasma hardened steels showed more hardness than laser hardened steels however in light of their examinations they found captivating results that laser hardening of 13Cr-4Ni steels indicated better disintegration protection at all edges of impingement than pulse plasma nitriding. Furthermore, it had been assumed that the measure of disintegration with erodent assess run 150-300 μm was two times more than the measure of disintegration with erodent measure go under 150 μm and SEM examination clearly revealed

that plastic distortion mode was in a general sense responsible for material departure in laser cemented steels.

Das et al. [17] concentrated the erosion wear of aluminum combination composites. The 21LM13 combination and LM13-Sic composites were produced to concentrate the results of sand fixation on the wear conduct in acidic and marine condition for a navigated separation of 763 km and a rotational speed of 900rpm. They watched that the wear rate increment with expanding sand fixation regardless of the material. This is on the grounds that as the convergence of sand in the slurry builds the seriousness of disintegration/rough assault increment in light of the fact that a more noteworthy number of particles are impinging at first glance. Then again, the slurry of erosion assault may diminish in light of the fact that the powerful volume of the corodent diminishes. The compound showed higher wear rate contrasted with the composite as sand fixation expanded from 0% to 40%. It was inferred that all the material showed higher wear rate in the acidic media when contrasted with NaCl at 0% and 20% sand fixation. However, at 30% and 40% sand focuses the material groups bring down wear rates in acidic media. The wear rate of the considerable number of materials diminished with separation crossed and approaches a consistent esteem. Notwithstanding, the wear rate of LM13-10% Sic composite expanded at first and after that lessening to this esteem. In acidic slurry, the wear rate of the combination ways to deal with pinnacle esteem and then decline to a steady esteem. In any case, the wear rate of the composites diminished monotonically with separation crossed and achieved a steady an incentive at a long testing time. They take note of that the mass misfortune rates of all material expanded when the speed was expanded from 700 to 900 rpm. This is on account of the vitality of impinging molecule is straightforwardly relative to the speed. At the point when the speed was expanded from 900 to 1100 rpm, the mass misfortune rate diminished regardless of the material and arrangement sort. This is on account of at higher speed the sand particles essentially slide over the surface as opposed to having any sensible effect.

Dube et al. [18] concentrated the impact of slurry turbulence on wear with a counter turning twofold circle erosion analyzer created by DUCOM. In this examination they utilize two circles (diameter 160mm and thickness 2mm) of aluminum and stainless steel (ss-304) put pivotally and turns at equivalent rate in inverse heading with the assistance of two enlistment engines. The plates are settled toward the finish of each of engine shaft. The separation between plates can be changed to

create the turbulence in slurry chamber. Silica and alumina are utilized for making slurry. The centralization of both the slurries differs from 14% to 55% in venture of 7% and keeping precise 1500 rpm and time consistent (1h). They found that wear increment with increment in molecule fixation (wt. division) the outcome demonstrates that wear increments straightly with molecule focus in all cases aside from wear on stainless steel by alumina. Alumina slurry demonstrates a slight decline in wear of stainless steel between 0.25 to 0.35 focuses. Amid test they established that the wear on stainless steel plate (ss-304) is less contrasted with aluminum in all the three parameters; time (0.5-3h), precise speed (1000- 3000rpm) and focus (14-55%). This is a result of high return quality of the stainless steel than aluminum. The centralization of slurries is taken as 40% and rakish speed fluctuates from 1000- 3000rpm. Then it was watched that expanded in the precise rate builds the turbulence and 22 henceforth increment in the weight reduction of plates. The impact of wear is higher in alumina slurry over the scope of rakish speed. The alumina slurry causes the higher volume misfortune then silica slurry indistinguishable testicles conditions since alumina is harder than silica particles.

Desale et al. [19] directed an examination to demonstrate the variety of erosion rate with introduction plot for strong fluid blend of three common erodent (quarts, alumina, and silicon carbide) for pliable target material AA 6063 and A1513042 steels the test performed in a pot analyzer pivoting example at 3 m/s in 10wt% concentrated slurry having molecule estimate 550 μ m. As the introduction edge increment then erosion rate Ist increment up to a most extreme and afterward abatements to a relentless state till 90°. Both the objective material shows greatest wear at shallow edges with every one of the three erodents. The maximum wear point seen as 15° and 22.5° for AA6063 and AISI 304L steel separately. At that point it reasoned that plot for greatest wear is an element of target material properties and don't rely on upon erodent properties.

Mishra et al. [20] concentrated every one of the parameters influencing the disintegration wear utilizing plane erosion analyzer on fly fiery remains quartz covering. By changing distinctive parameters, they assessed that effect edge is the most critical component affecting the erosion wear of fly fiery remains quartz covering. They additionally assessed that most extreme erosion happens at effect edge of 90°.

Neville et al. [21] concentrated the erosion erosion conduct of WC-Metal Matrix Composites (EFM, EFW, EGC, EGG). The materials were dissolved by two sizes of silica sand with stream speeds of 10 and 17 m/s at 65°C. Test was directed by differing the fixation. They evaluated that WC grain measure divisions has almost no impact on wear. They likewise inferred that the erosion–consumption rate is unequivocally reliant upon erodent measure, impinging speed and strong stacking.

Modi et al. [22] concentrated the erosion of high carbon steel in coal and base powder slurries with 30% focus and 5m/s test rotational speed. It is watched that weight reduction of H.C. steel example increment with increment in traversal remove 30% concentrated slurries of water +bottom powder and water + coal. The test is directed on both hardened and annealed steel for same exploratory conditions. At first the rate of increment in loss of material was essentially high. Example accomplishes a steady–state wear condition on further increment intraversal remove. At longer traversal separate distinction between wear of tempered example because of coal slurry and base fiery debris slurry decreases. It is watched that weight reduction of strengthened steel was almost 10 times all the more then solidified steel in both slurries with 30% focus and 5 m/s test rotational speed. It is watched that higher material loss of steel tests (Both tempered and solidified) in base cinder slurry than in coal slurry has been brought about by the nearness of a vast amount of harder mineral constituents and less breaking inclination of coal slag particles. The coal fiery debris particles are gentler and furthermore get break amid the procedure of erosion bringing about little bits of diminished active vitality.

Walker and Bodkin [23] tried wear rate of side liner material (cast press) on three gatherings (STD, HE and RE) at two tip speeds each with 1000µm sand particles size of 0.3 (by volume) concentration slurry. Speed did not demonstrate any checked impact on side liner wear rate, with the RE Impeller demonstrating a slight increment and the HE a slight lessening with expanding speed. They likewise observed that impact of sand molecule measures on side liner material (cast press) wear was not noteworthy for STD impeller. They likewise watched that wear rate for molecule measure 150µm, 500µm, 1000µm was almost same. Be that as it may, for the gathering it was the prevailing variable. The wear rate is corresponding to molecule measure.

Walker [24] thinks about the wear rate after effect of lab test and field test on side liner of STD and HE setups of impellers. He found that the lab wear rate with cast iron material was more noteworthy than the wear rate for the field comes about with the white cast iron because of hardness of parts. Both material show magnificent likenesses in wear rate drift with molecule measure. It is found from field result that elastic show brings down wear rate than the metal for proportional molecule estimate $< 700\mu\text{m}$. This is on account of the elastic surface can assimilate littler molecule impact energy without huge cutting tearing.

Singh and Gandhi [25] has directed investigations in a pot analyzer for breaking down the impact of introduction of plane surface in respect to its movement in strong fluid suspensions. They directed analyses at different working conditions by fluctuating the effect point, characterized as the angle between the digression to the plane surface and its speed. Level metal test pieces flush with a surface of solidified carbon steel plate (hardness= RC45) were taken. The introduction or effect edge was differed from 0° to 90° and focus range was 20-40%. It has been discovered that the disintegration wear diminishes with increment in introduction point yet this lessening was not reliable. It was seen that wear increments with the expansion in introduction edge till 30° and after that abatements with increment in introduction point up to 90° for different scope of speeds and molecule sizes. Promote it has been presumed that wear at 30° edge was 3-4.5 times higher than at 90° introduction point and furthermore wear increments with increment in speed and molecule estimate yet diminishes with increment in strong focus under various effect edges.

Harry and Graeme [26] directed test on erosion wear of delicate malleable aluminum compounds and hard fragile high chromium white iron utilizing coriolis wear test with slurries of various solids and focus. The aluminum combinations tried were A380 (a kick the bucket cast grade) and 6061T-6511(an expelled review). The high-Cr white irons were high-Cr press (sand cast) and G75 high-Cr (radiating cast). The measurement of test example was $63.5\text{mm}\times 19.1\text{mm}\times 6.4\text{mm}$. The test slurry was made up of grades of silica carbide sand and clean water. A few molecule sizes were utilized as a part of the tests with mean measurement extending from $22\mu\text{m}$ to $1428\mu\text{m}$. Solids particles were semi-adjusted to semi-rakish shape. Coriolis destroy tests were conveyed at encompassing temperature with the speed of 975 rpm. They watched that higher the strong volume part the all the more as often as possible and unequivocally the solid particles contact with the objective material, and results in more wear. It was presumed that when slurry focus increment

from 1.52 vol.% solids to 12.12 vol.%, the wear rate expanded material made up of high-Cr (sand cast) and on the aluminum compound. It was watched that bigger strong particles brought about high mass misfortune in the materials tested. The slurry with solids focus of 12.12 vol.% and flow rate of 15 gal/min, the wear rate expansion for the aluminum composites is around 20–28 times and for the materials of white iron is around 42–45 times as the mean width molecule measure expanded from 22 μm to more than 1400 μm . At 22 μm (D50), the difference in wear rate was about 4.3% between G75 white irons and high- Cr (sand cast), and less (-) 6.7% between the 6061T-6511 and aluminum amalgams 380. The rate of wear contrast developed to 29.9% between the aluminum amalgams and 10.3% between the white irons at the 1428 μm (D50) molecule size. It was likewise found that the wear rate proportion between the white iron G75 and aluminum compound 380 was around 40 when tested with fine particles (22 μm D50). Wear proportion esteem crested nearly 150 with molecule measure in the range of 100–200 μm and diminish to nearly 27 with size of 1400 μm extremely coarse particles. During the test it was found that a higher slurry stream rate produces more erosion wear yet the wear rate increment wasn't as high as stream rate increment. They watched that the considerably harder and more grounded white irons of high-Cr demonstrated a colossal favorable position in wear resistance(upto150times) over the test aluminum combinations in test condition. Since Among the test materials, the expelled aluminum amalgam containing constrained combination components has the most noteworthy elongation/ductility.

Machio et al. [27] has concentrated the erosive wear of WC–12 wt.%Co and WC–17 wt.% Co and in addition trial WC–10 wt.%VC–12 wt.%Co and WC–10 wt.% VC–17 wt.%Co coatings stored on stainless steel substrates utilizing a high weight high speed oxy-fuel (HP/HVOF) warm showering framework. The slurry comprised of the silica carbide sand with water. The impeller circled the slurry through a spout of distance across 12.5 mm. Tests were led at 45 and 90 frequency edges on examples of size 50mm \times 50mm \times 6 mm. The outcomes demonstrate that the WC–VC–Co coatings show higher disintegration resistance then business WC-Co coatings. In slurry disintegration, the best execution of the VC-containing coatings is on a par with that of the business WC–Co coatings. They found that the disintegration resistance of the WC–VC–Co coatings was like that of the business grades. This might be expected to the (V, W) C grains being less impervious to effect crack as a result of their higher hardness.

Chapter 3

PROBLEM FORMULATION

The martensitic chromium stainless steel (13/4 or CA6NM steel) has wide application in hydro turbines, pumps and compressors. But it has following limitations:

- Less resistance to erosion
- Poor mechanical properties of weld joint and repair welding

Since replacement of eroded runner assembly is very costly, weld repair of the runner assembly is a feasible option. During the various studies, it was observed that the performance of the welded runner assemblies is not satisfaction and fail prematurely, possibly due to the poor weldability of the martensitic steel. To overcome the problem of erosion and poor weldability, an erosion resistant material was developed for the fabrication of the underwater parts of hydro turbines i.e. Nitronic steel (21-4-N and 23-8-N steels). But the erosion resistance of the welds of the Nitronic steel is still under consideration because nitrogen content in the weld and matching filler.

So in this background the weld beads of 21-4-N and 23-8-N Nitronic steel in As Cast condition with GMAW welding using ER2209 filler wire and pure argon as shielding gas are to be tested with jet type slurry erosion machine and the erosion resistance of the welds of this material to be studied.

So the basic objective of this work is to do study of the erosion wear of the welds of this material and study the effects of various parameters (impingement angle, time, etc.) on erosion wear of the welds.

Chapter 4

EQUIPMENT, MATERIALS, EXPERIMENTAL PROCEDURES

4.1. BASE MATERIAL PROPERTIES

Experiments are conducted on the 21-4-N and 23-8-N steels in As cast conditions. Large plates of 100 mm × 100 mm cross-section are received from M/s Star Wire (India) Ltd. Ballabhgarh (Haryana).

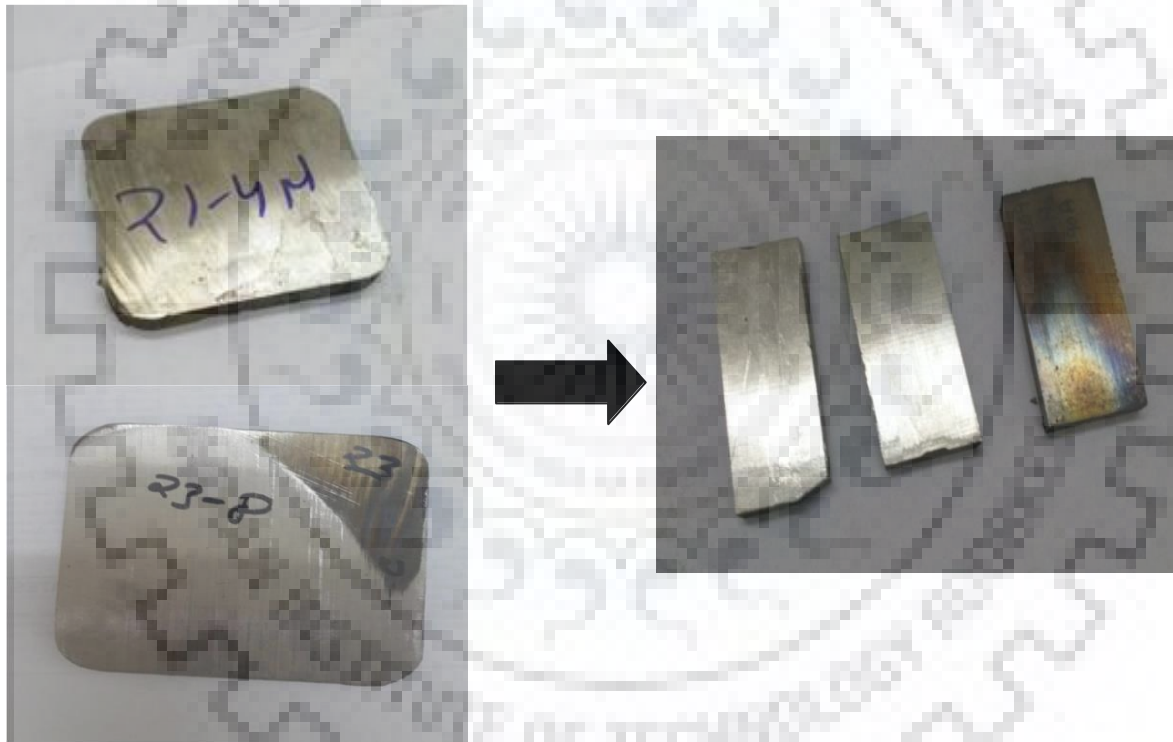


Fig 4.1: Nitronic steel (21-4-N and 23-8-N steel)

4.1.1. Chemical Composition

Table 4.1: Chemical composition of the 21-4-N Nitronic steel (wt.%) [28]

Steel	C	Mn	Si	Cr	Ni	N	Cu	Fe
21-4-N steel	0.48 – 0.58	9.9	0.25	21.0	4.0	0.38	0.3	Bal.

Table 4.2: Chemical composition of the 23-8-N Nitronic steel (wt.%) [28]

Steel	C	Cr	Ni	Mn	N	Si	Mo	S	P	Fe
23-8-N steel	0.34	22.60	7.55	2.12	0.29	0.78	0.20	0.001	0.037	Bal.

4.2. WELDING

4.2.1. Welding Process

The large base metal plates are first cut into small plates of 75 mm × 25 mm cross-section. The welding process chosen is Gas Metal Arc Welding (GMAW) process as it is best suited for thick materials with highest weld quality. It is widely used for stainless steel welding. In the given study manual GMAW is used for weld bead on 6 mm thick base metal plate. The welding is successfully completed at welding research laboratory IIT Roorkee.

Table 4.3: Welding number as per filler and shielding gas used

Weld	Filler	Shielding gas
Weld bead	ER 2209	Pure Argon

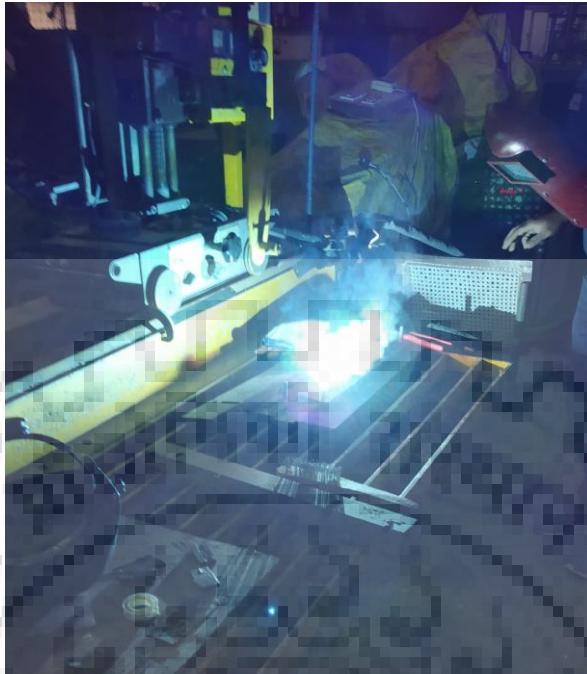


Fig 4.2: GMAW welding



Fig 4.3: Welded Sample

4.2.2. Welding Parameters

The welding parameters are chosen on the basis of previous study done on weldability of nitronic steel. The nitrogen content in shielding gas increases the content of nitrogen in the weld.

Table 4.4: Welding Parameters

Welding Current	110 - 120 Amp
Voltage	23
Gas flow of Ar	10 L/min
Filler wire diameter	1.2 mm
Welding speed	160 mm/min

4.2.3. Filler Metals

There is no commercially available filler metal for nitronic steel. However, a successful attempt has been made to join these steel by commercially available stainless steel electrodes. But the mechanical properties of these welds are inferior as compared to the base metal properties. Thus, an effort is needed to select the filler material in such a way that the weld metal should have approximately same composition and mechanical properties comparable to base material.

The filler material for nitronic steel should:

- Resist to hot cracking
- Provide adequate mechanical properties of weld metal
- Sustain the nitrogen content level in the weld metal

Table 4.5: Chemical composition of filler metal

Filler Metal	C	Si	Mn	Cr	Ni	Mo	Cu	N
ER2209	>0.03	0.52	1.71	22.51	8.53	3.34	<0.3	0.16

Table 4.6: Mechanical properties of filler metal

Filler metal	Ultimate tensile strength (MPa)	Yield Strength (MPa)	Impact Energy (J)	Ductility (% elongation)
ER 2209	670	560	100	26

4.3. HARDNESS TESTING

Hardness is the measurement of a material to resist indentation or penetration, to resist abrasive wear when a compressive force is applied. The hardness testing is done on OMNITECH micro hardness tester model MVS-S-AUTO.

The polished samples of welded joint are tested with following specifications:

- Indentation load: 300 grams
- Dwell time: 10 seconds

The hardness is measured at 1 mm spacing between each indentation. The result shows that the base metal is having hardness more than the weld beads. The reason for high hardness is the presence of nitrogen and carbide in the structure. The hardness is increased as the nitrogen content is increased.



Fig 4.4: Hardness testing setup

4.4. EROSION WEAR STUDY

Erosive wear study is conducted on the je-type slurry erosion test machine available in welding research laboratory IIT Roorkee. The setup includes erosion chamber, propellers, propeller housing and mixing tank are made with AISI 304-L stainless steel as they can be affected by corrosion-erosion conditions and other parts are made from mild steel. The propeller housing is fitted with ceramic ball bearing on both sides to support propeller shaft. The machine is supplied with 2HP single phase A.C. motor to drive the mixer propeller at constant speed of 1500 rpm for the proper mixing of sand and water. This uniform mixture is pumped into piping system by a special centrifugal slurry pump of 0.5 HP and a discharge of 2 liters per second.

The impellor is made of hardened white cast iron and the casing is made of AISI 316-L with rubber lining for erosion-corrosion resistance. The function of pump is only to provide a necessary motion to slurry and the main propulsion is obtained by compressed air which is expanded inside the chamber of specially fitted Y-geometry attachment. On expansion inside the chamber of Y-geometry attachment work is done on the slurry which is propelled through a convergent-divergent nozzle. As the slurry passes through the 6 mm diameter it attains very high velocity which is enough to cause the erosion of materials. Inside the erosion chamber a portable vice is fitted to clamp the holders. These holders are prepared to fix the samples at different impact angle during slurry erosion testing.



Fig. 4.5: (a) Front view (b) Side view (c) Close view of Jet-Type Slurry erosion test machine

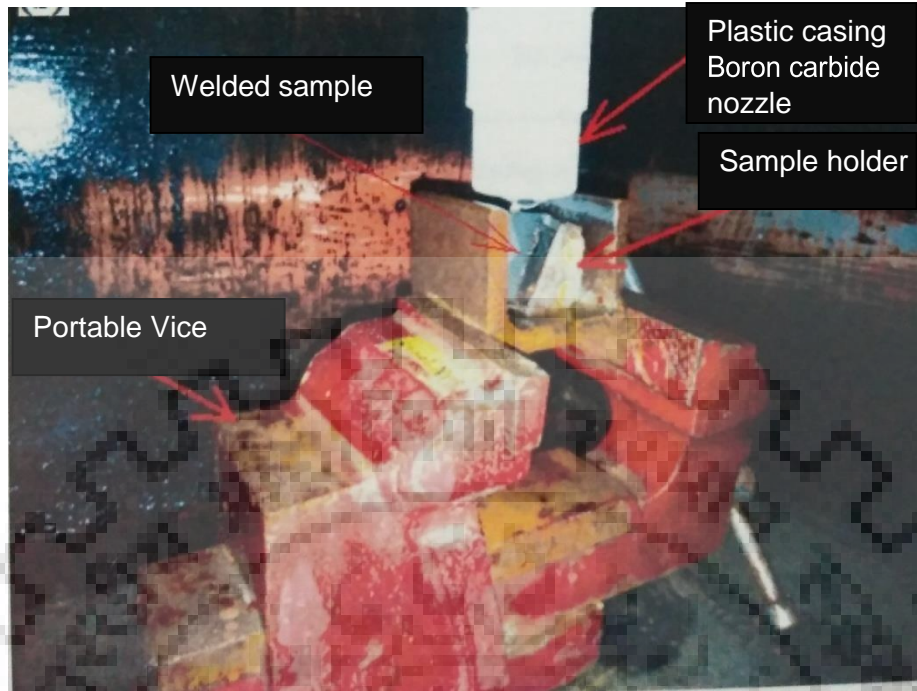


Fig. 4.6: Sample orientation

The erosion testing has been conducted as per the test parameters listed in table: Prior to the testing, the welded specimens were cleaned with acetone, dried with hot air and finally weighted to 0.1 mg precision. During the testing, the welded specimen was exposed to a slurry-jet composed of water and silica sand (SiO_2) particles as shown in figure. After the erosion testing, the samples were removed from the fixture, cleaned with acetone, dried with hot air, and finally weighted again to measure the material loss.

Table 4.7: Erosion Parameters

TEST PARAMETERS	VALUES
Erodent size and material	100-500 μm , SiO_2 particles
Erodent velocity (m/s)	18.5
Impact angle (degree)	30, 60 & 90
Slurry Concentration (wt. %)	10
Nozzle diameter (mm)	6
Nozzle to workpiece distance (mm)	10
Test time (minutes)	30, 60 & 90

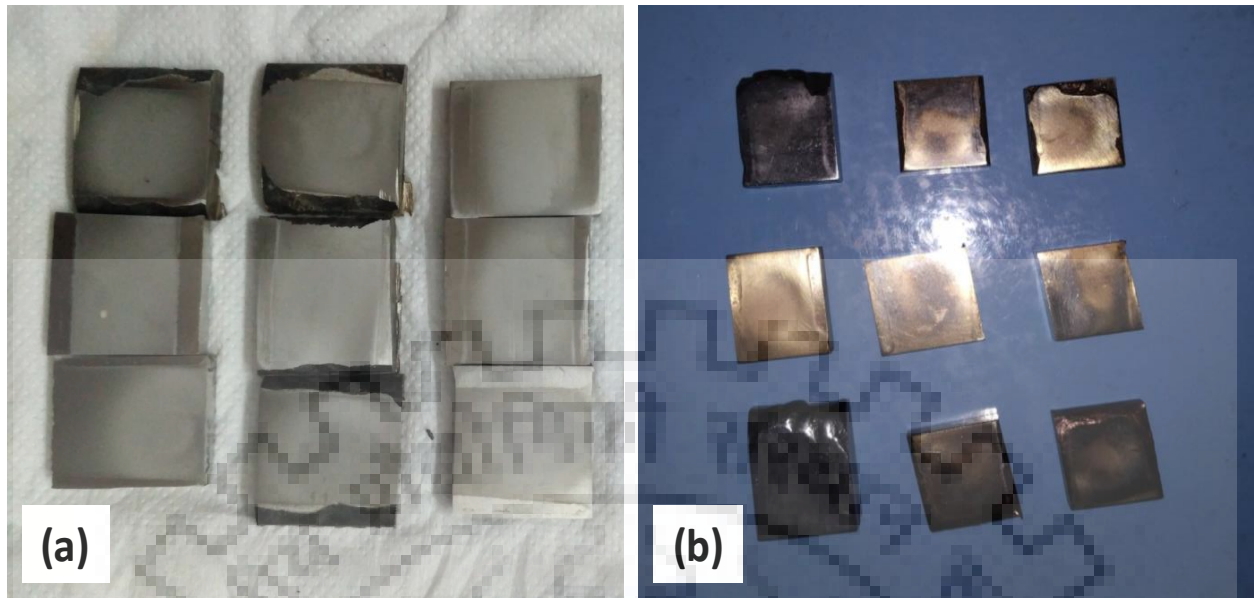


Fig 4.7: Samples after Erosion testing (a) 21-4-N and (b) 23-8-N

4.5. FE-SEM

In FE-SEM emitted electrons are used for surface characterization of welded samples. The Welded samples were placed in vacuum chamber where high vacuum was maintained and then 20 KV applied between anode and cathode for emission of electron. These emitted electrons are deflected and focused on very small spot of nm size on surface. Higher magnification was used ranging from 500X to 5000X (500X, 1000X & 5000X).



Fig. 4.8: FE-SEM machine

Chapter 5

RESULTS AND DISCUSSIONS

5.1 MICROSTRUCTURAL EXAMINATION

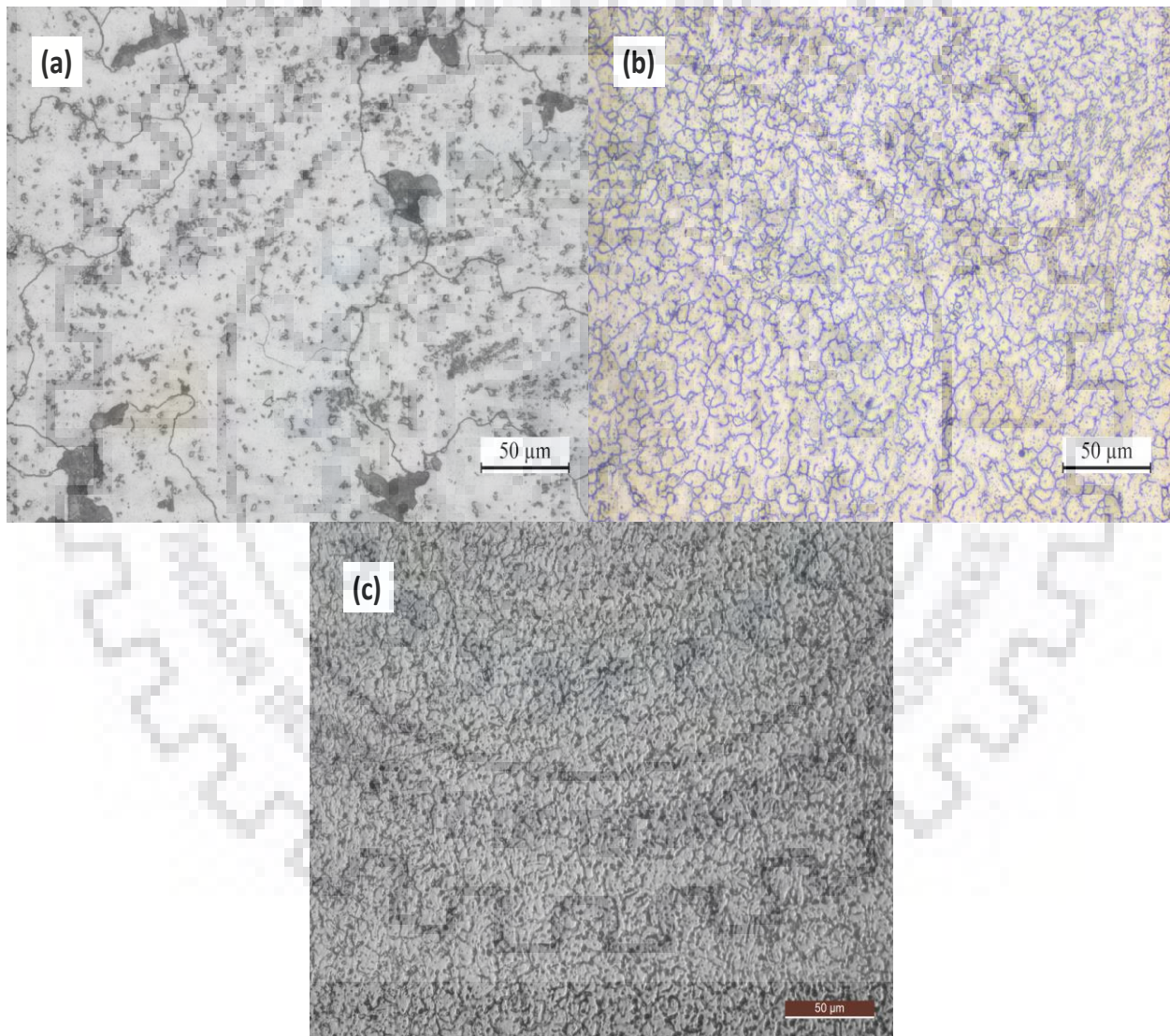


Fig. 5.1: 21-4-N (a) Optical micrograph of base metal, (b) Optical micrograph of As weld, and (c) Optical micrograph of weld with quench

The optical image analysis at 200X magnification is done on the three samples namely (21-4-N steel) base metal, As weld and weld with quench have been shown in the above figure. The base metal is fully austenitic structure, As weld has some ferrite and fine grain structure austenitic structure. And austenitic structure with more ferrite in weld with quench.

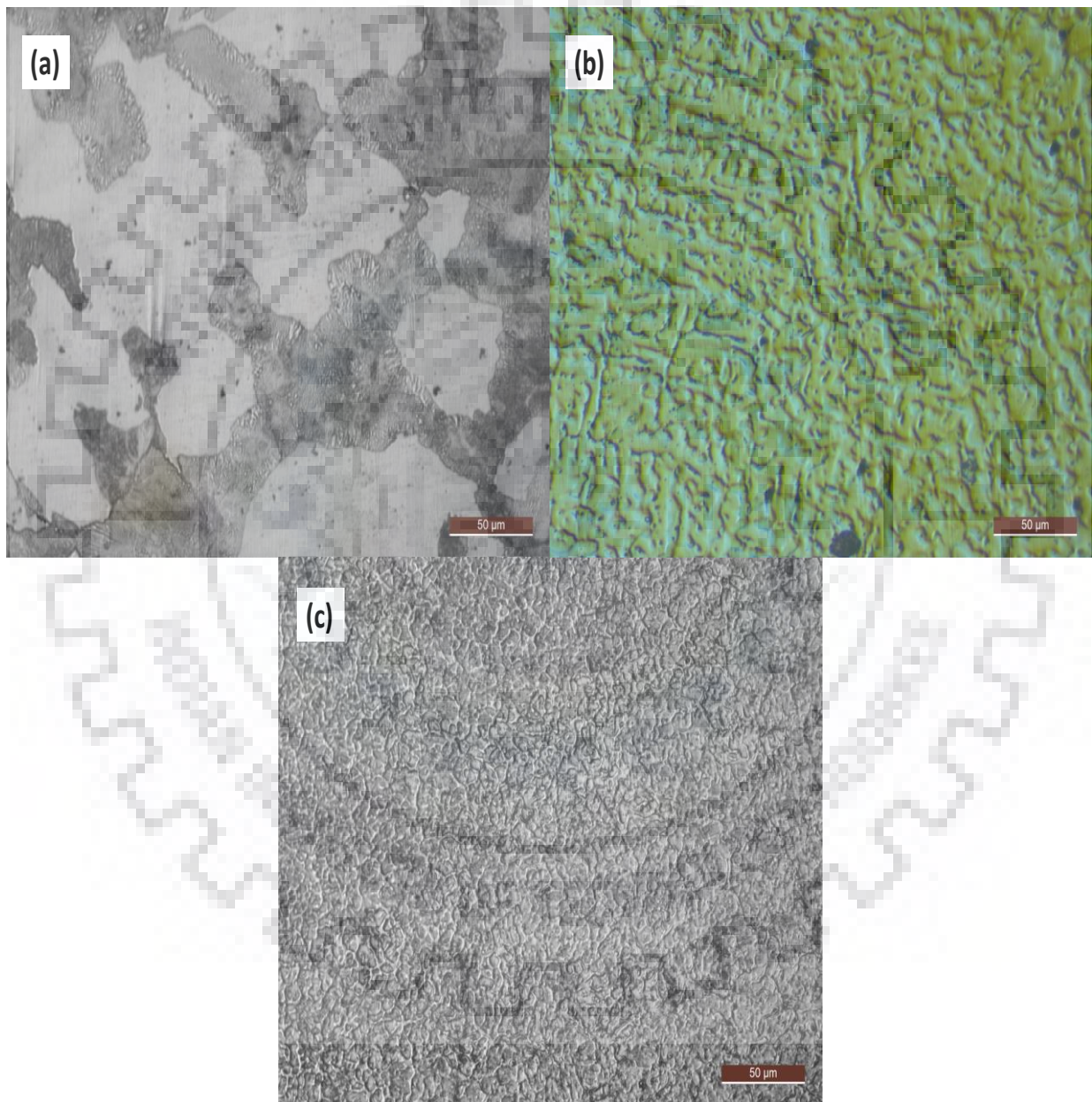


Fig 5.2: 23-8-N (a) Optical micrograph of base metal, (b) Optical micrograph of As weld, and (c) Optical micrograph of weld with quench

The optical image analysis at 200X magnification is done on the three samples namely (23-8-N steel) base metal, As weld and weld with quench have been shown in above figure. The base metal is fully austenitic structure, As weld has some ferrite and fine grain structure austenitic structure. And austenitic structure with more ferrite in weld with quench.

5.2 HARDNESS TESTING

Fig 5.4 shows the hardness of the samples plotted on the graphs. The three curves represent results for the different specimens namely 1 (base metal i.e. 21-4-N), As weld (weld bead on base with pure argon shielding gas), Weld with quench (quenching done after weld bead on base with pure argon shielding gas).

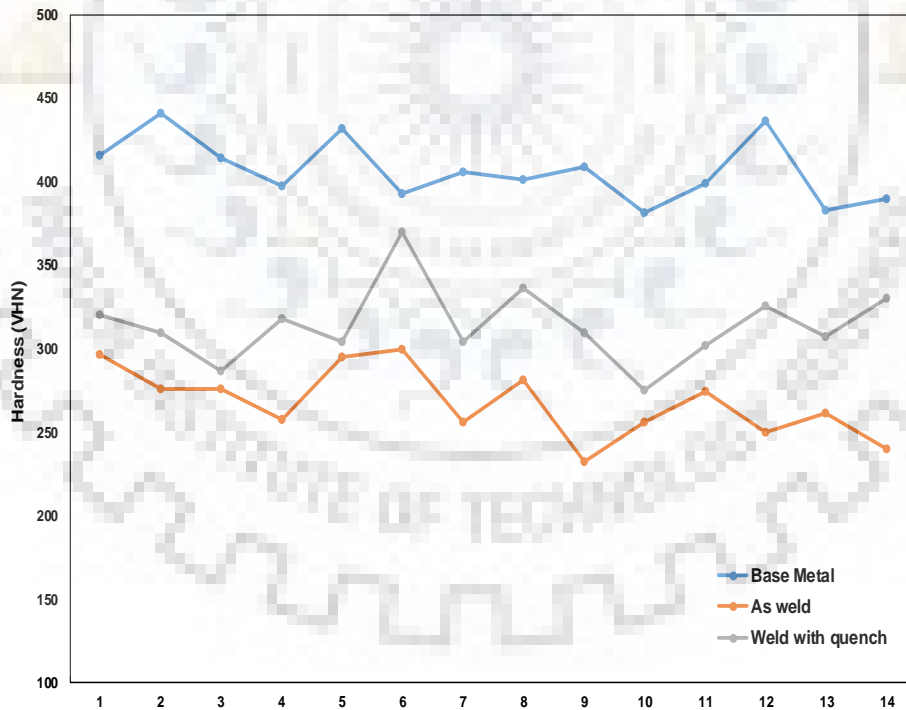


Fig. 5.3: Hardness profiles of 21-4-N base metal, As weld and weld with quench as a function of distance (mm) (plotted on x-axis).

Fig 5.4, shows the hardness of the samples plotted on the graphs. The three curves represent results for the different specimens namely 1 (base metal i.e. 23-8-N), As weld (weld bead on base with pure argon shielding gas), Weld with quench (quenching done after weld bead on base with pure argon shielding gas).

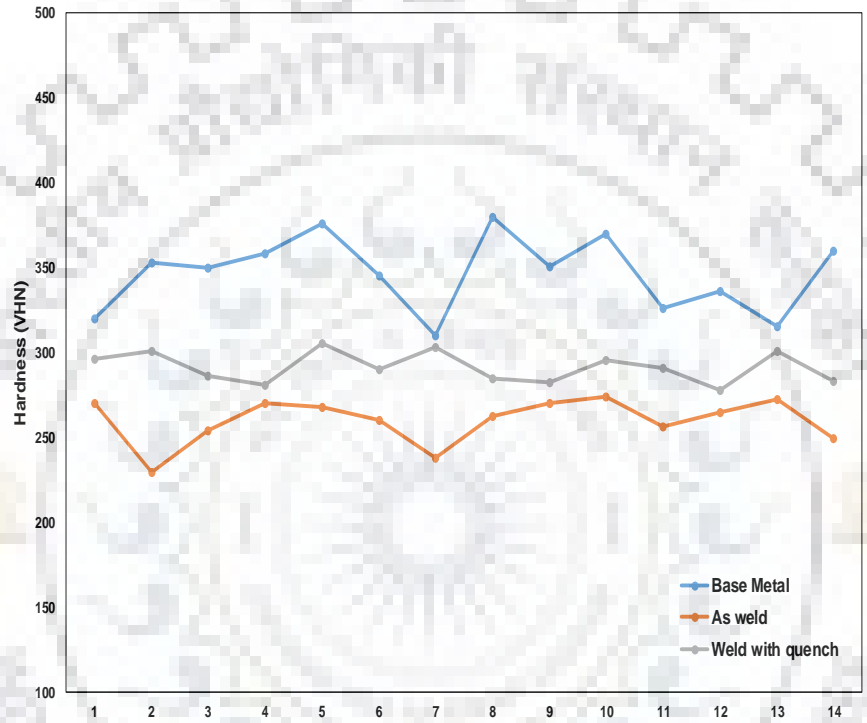


Fig. 5.4: Hardness profiles of 23-8-N base metal, As weld and weld with quench as a function of distance (mm) (plotted on x-axis).

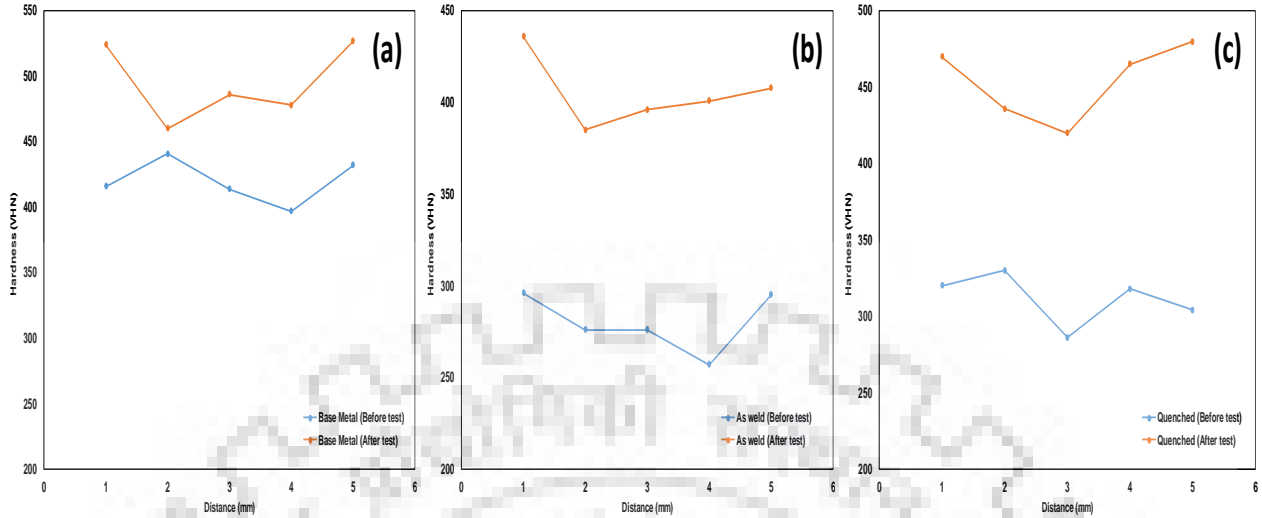


Fig. 5.5: Hardness profiles of 21-4-N (a) base metal, (b) As weld and (c) weld with quench as a function of distance (mm) (plotted on x-axis) before and after test.

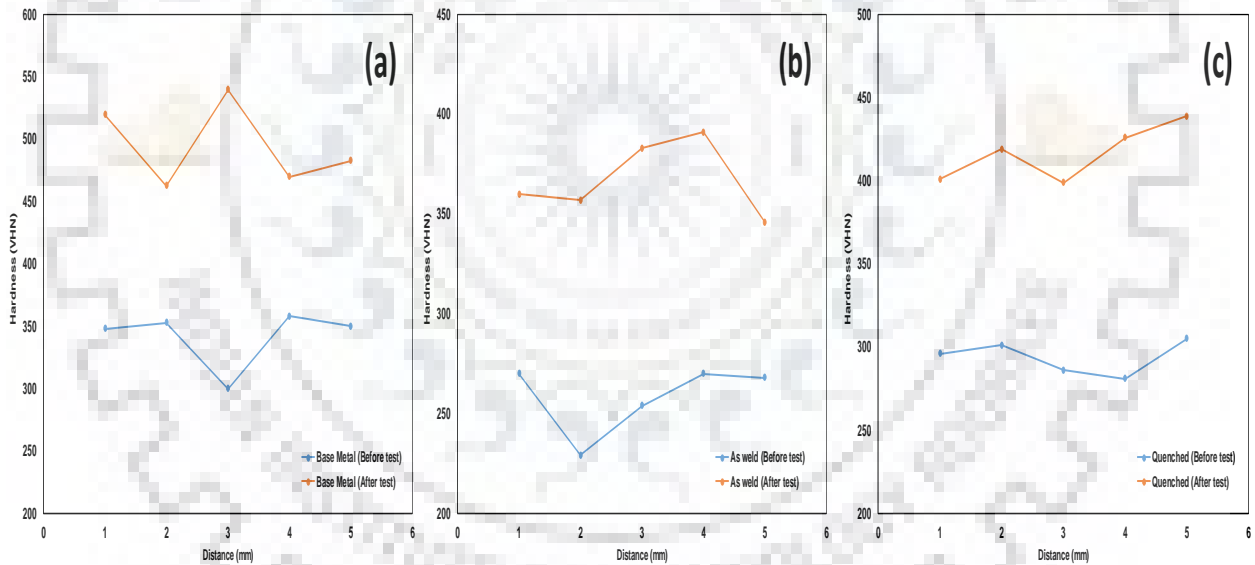


Fig. 5.6: Hardness profiles of 23-8-N (a) base metal, (b) As weld and (c) weld with quench as a function of distance (mm) (plotted on x-axis) before and after test.

The hardness testing of the base metal and weld metal are carried out with 300 grams load and 10 sec dwell time. The results are shown in the graphs. The reason for sample 1 and 4 has high hardness than their welds due to the low strength of filler metal ER-2209 used.

5.3. EFFECT OF TIME ON EROSIWE WEAR RATES

The effect of time on erosion wear was determined by calculating the cumulative weight loss of specimen. To understand the effect of time on erosion wear graphs were plotted between cumulative weight loss and time at angles of 30° to 60° to 90°. The erosion wear test duration was 30 min., 60 min., 90 min. It can be clearly seen in graph that amount of material loss increase with time.

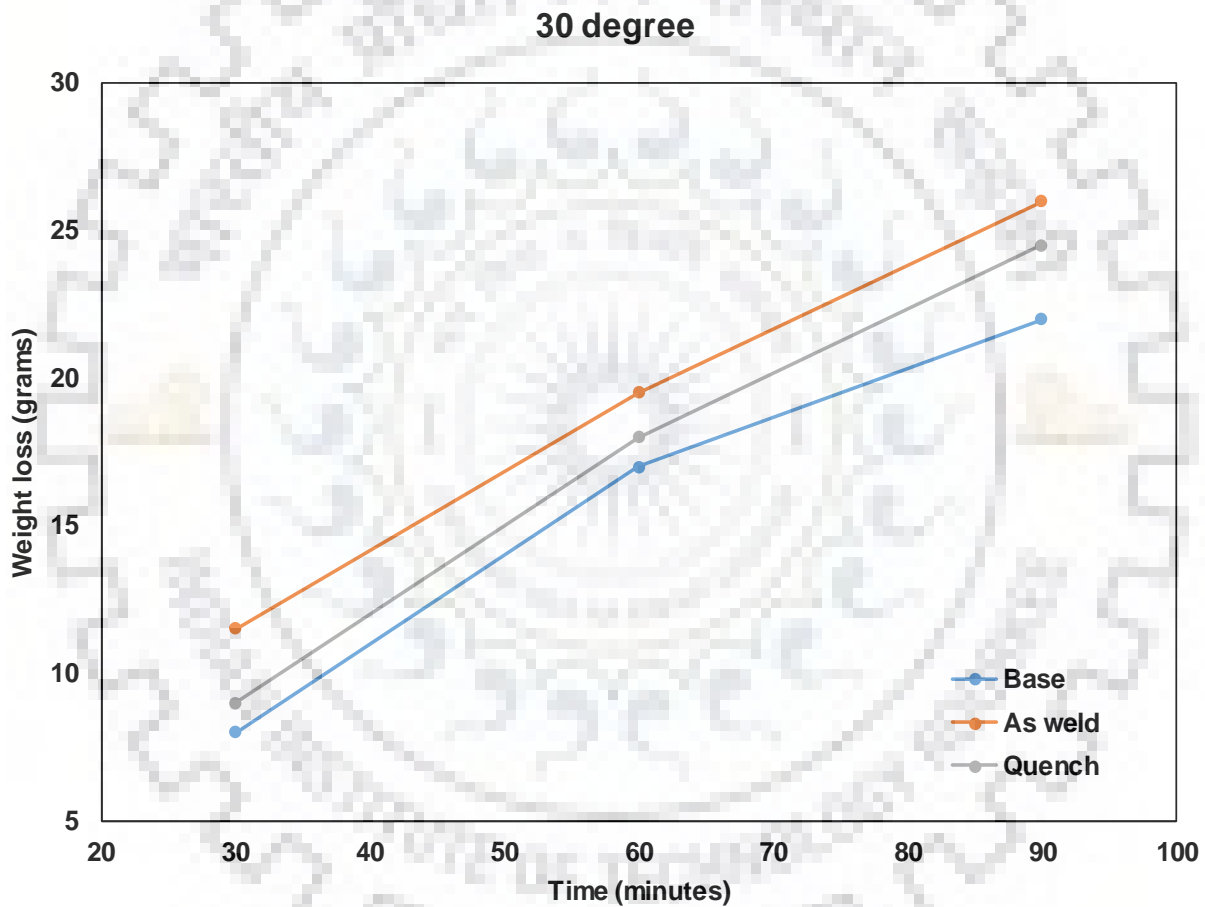


Fig. 5.7: Variation in cumulative weight loss with respect to time at 30° impact angle (23-8-N).

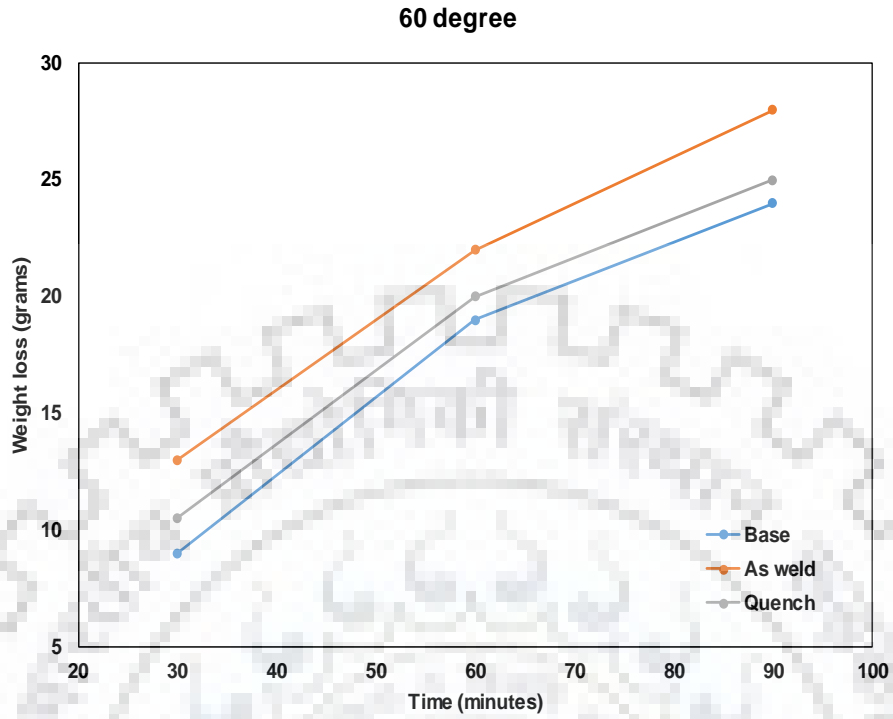


Fig. 5.8: Variation in cumulative weight loss with respect to time at 60° impact angle (23-8-N).

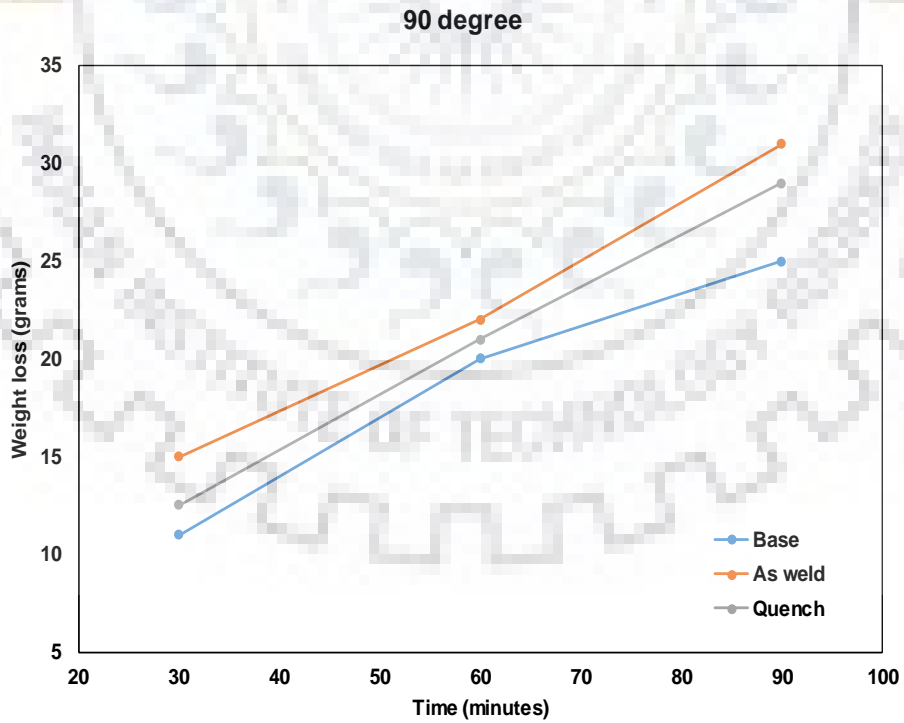


Fig. 5.9: Variation in cumulative weight loss with respect to time at 90° impact angle (23-8-N).

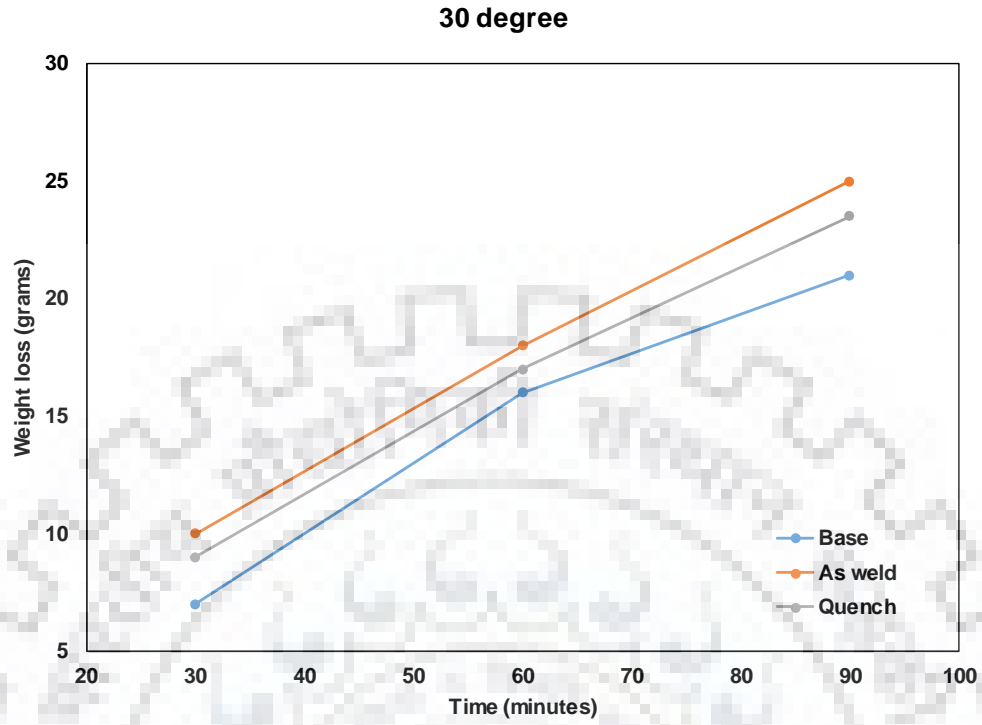


Fig. 5.10: Variation in cumulative weight loss with respect to time at 30° impact angle (21-4-N).

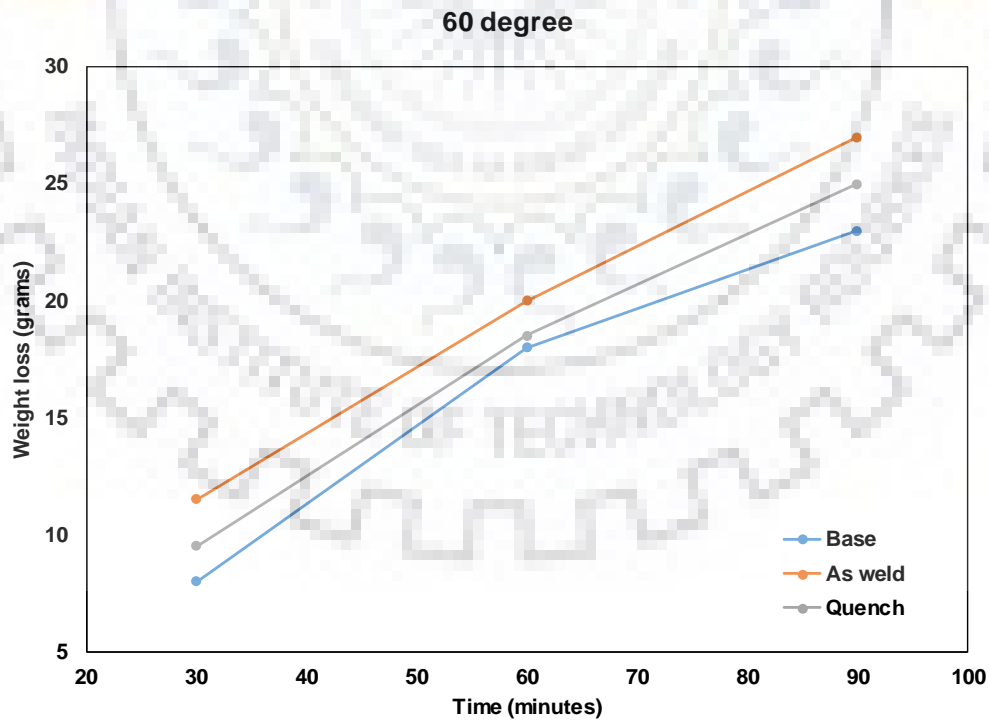


Fig. 5.11: Variation in cumulative weight loss with respect to time at 60° impact angle (21-4-N).

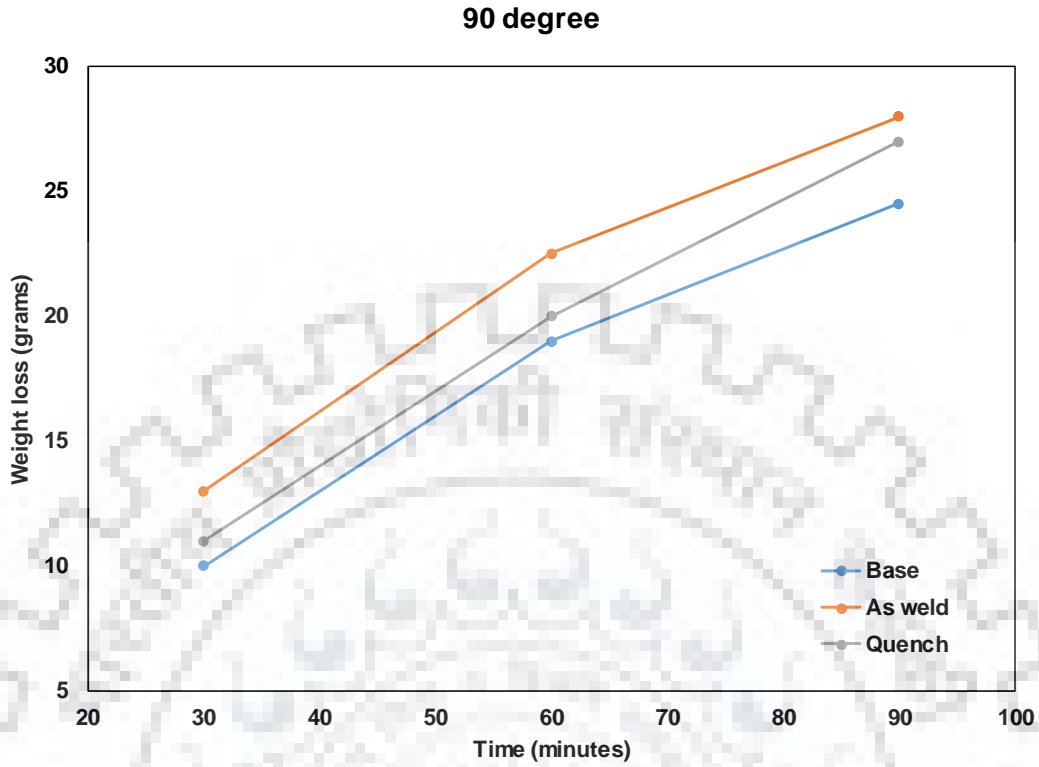


Fig. 5.12: Variation in cumulative weight loss with respect to time at 90° impact angle (21-4-N).

5.4. FE-SEM ANALYSIS

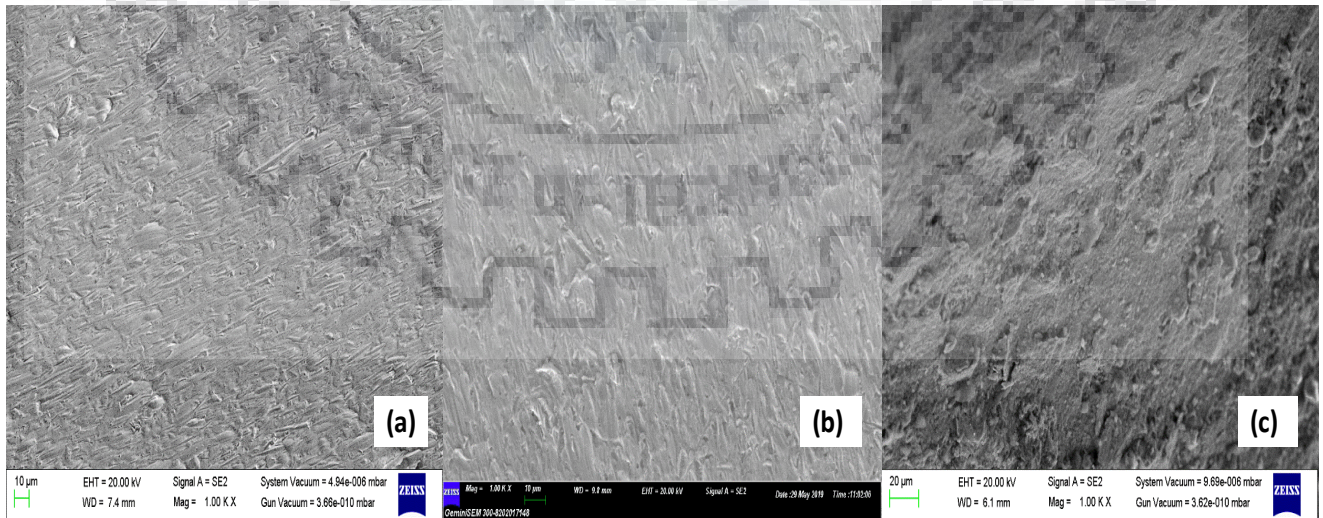


Fig 5.13: Base metal (21-4-N) (a) 30 degree, (b) 60 degree, and (c) 90 degree

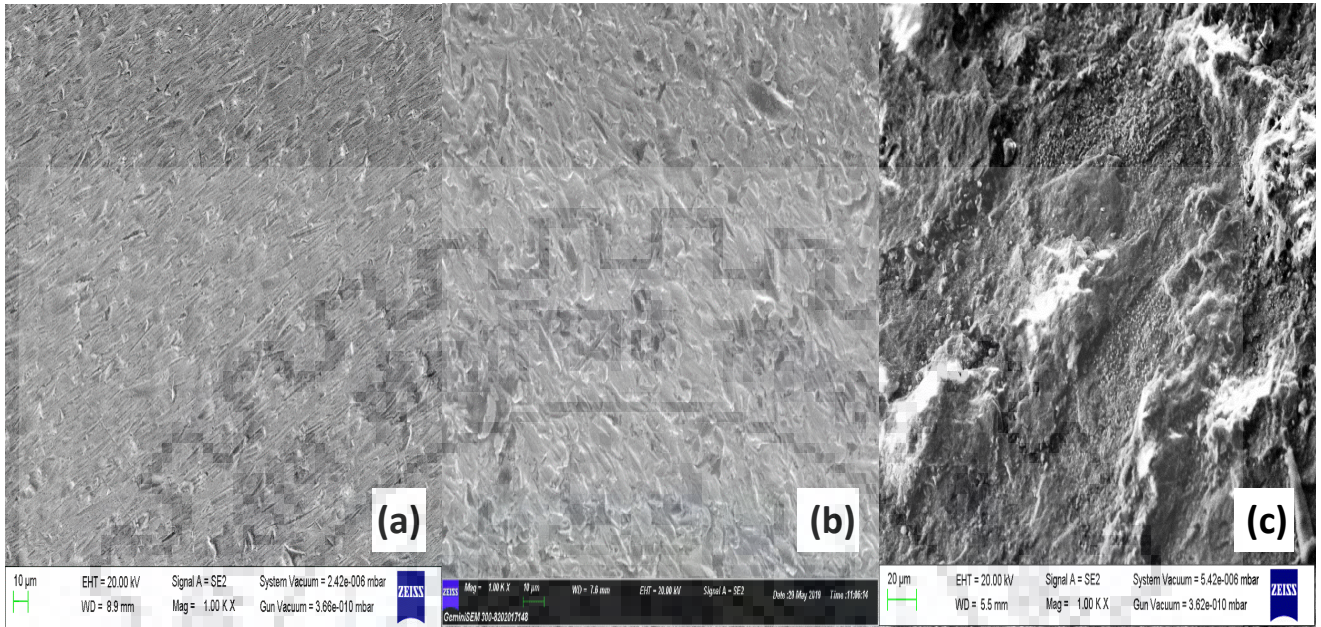


Fig 5.14: As weld (21-4-N) (a) 30 degree, (b) 60 degree, and (c) 90 degree

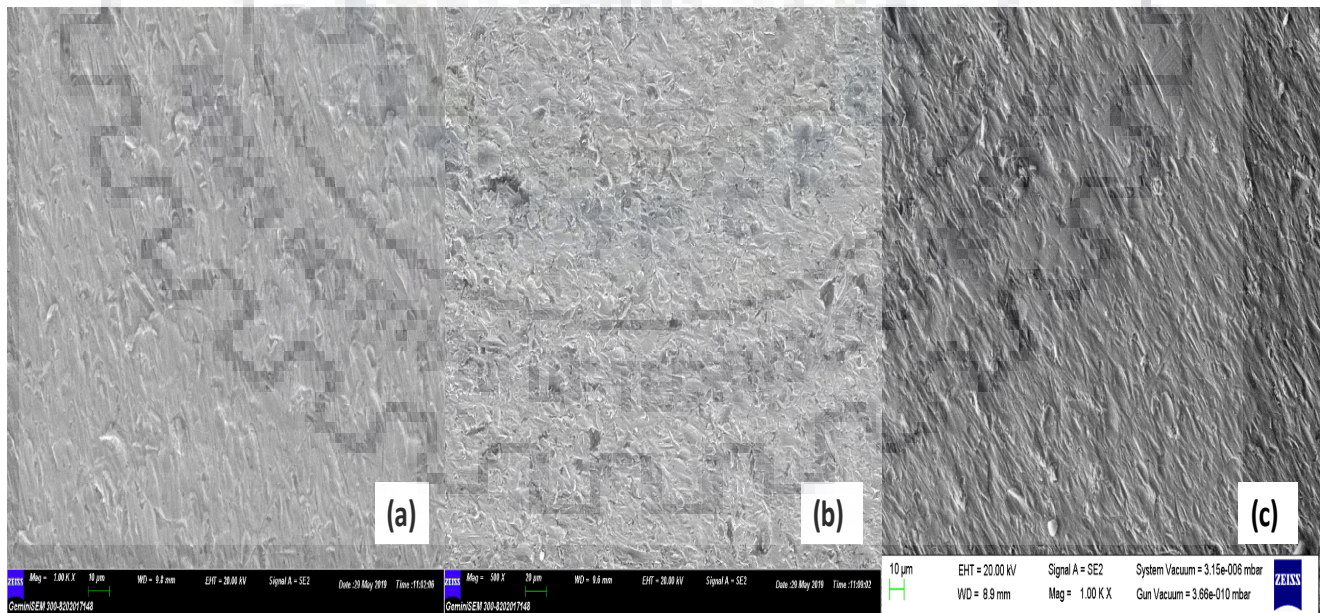


Fig 5.15: Weld with quench (21-4-N) (a) 30 degree, (b) 60 degree, and (c) 90 degree

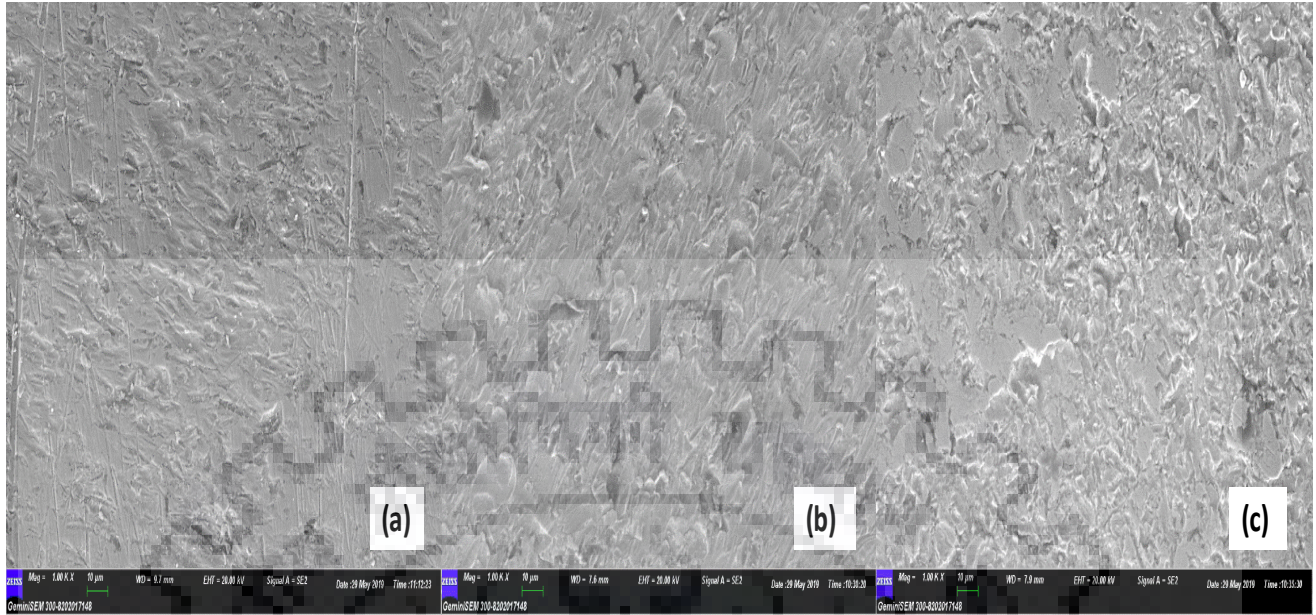


Fig 5.16: Base metal (23-8-N) (a) 30 degree, (b) 60 degree, and (c) 90 degree

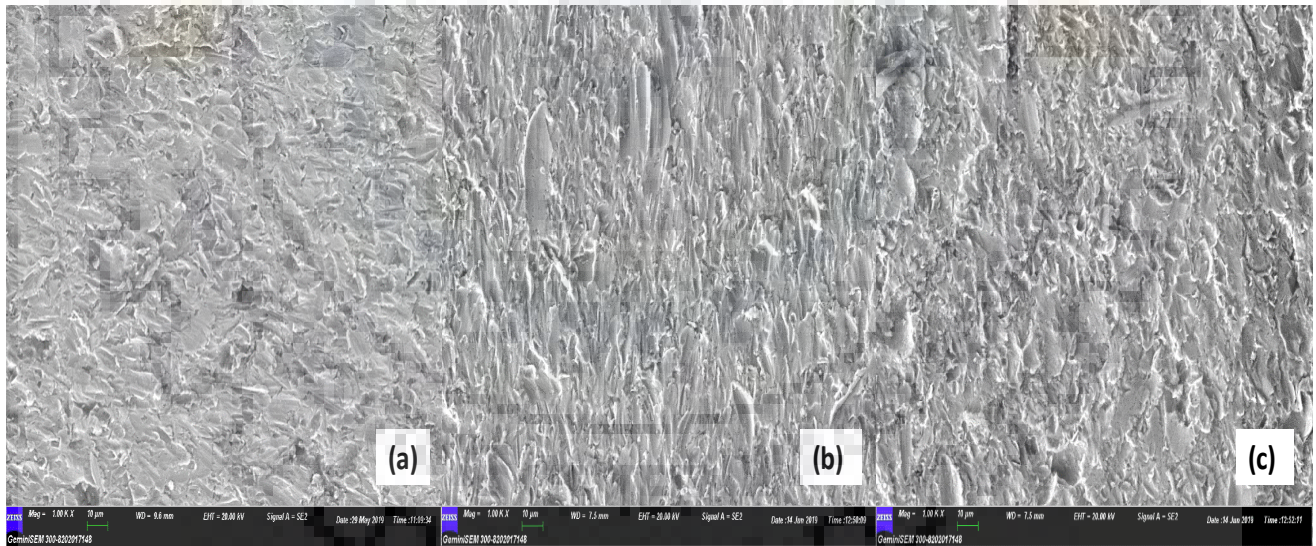


Fig 5.17: As weld (23-8-N) (a) 30 degree, (b) 60 degree, and (c) 90 degree

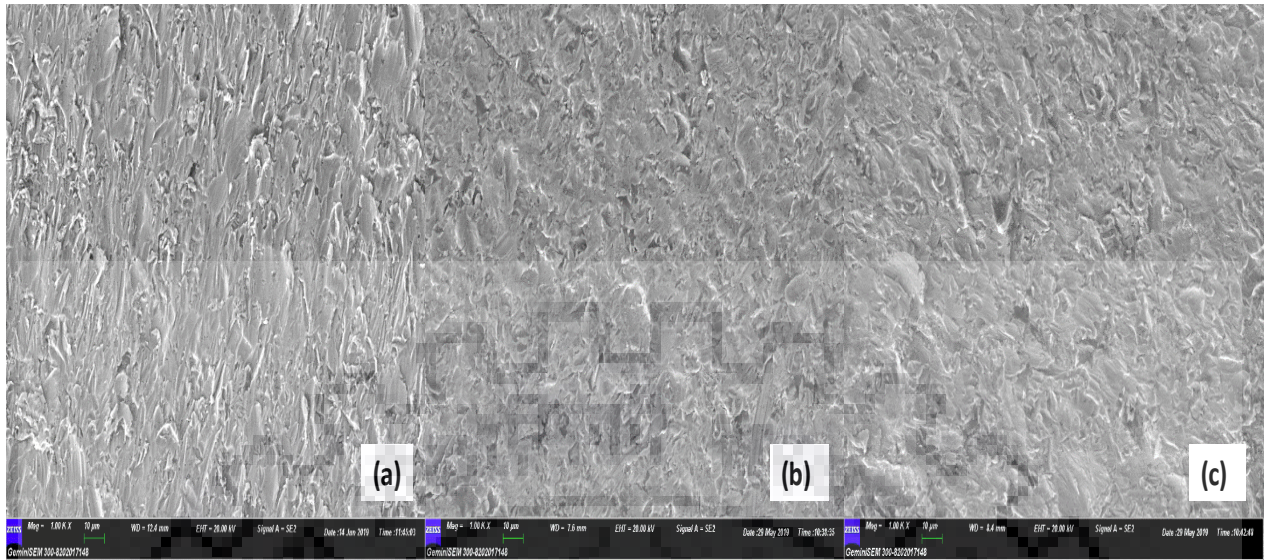


Fig 5.18: Weld with quench (23-8-N) (a) 30 degree, (b) 60 degree, and (c) 90 degree

The FE-SEM images of the samples were taken at 1000X magnification and it was seen that the mechanism of wear changes as the angle of impingement changes because of that the pattern in SEM images was different for the three images taken for each sample at angles of 30°, 60° and 90°. At 30° impingement angle the erosion loss is primarily due to shear cutting of surface material, whereas at 90° impingement angle resultant erosion damage is due to strain hardening and embrittlement of target material. Further the base metal, As weld and weld with quench shows the increase in erosion when angle of impingement is increased from 30° to 90° which is evident from SEM images as the differences in crest and trough were more in 90° sample as compared to 30°.

Chapter 6

CONCLUSION

Wear is one of the most common problems encountered in hydro turbine blades in hydro power plants in which solid liquid mixture is comes in contact with the blades of turbine. The base material 21-4-N and 23-8-N steel and its weld bead of As weld and weld with quench with GMAW welding with ER2209 filler metal with pure argon as shielding gas were taken for the study of erosion wear. The erosion wear evaluated with varying the parameters impact angle and time of erosion using jet type slurry tester as test apparatus. Weight loss of specimens is the measure of erosion wear. The conclusions of the experimental work are listed below:

- Maximum erosion wear was reported at 90° impact angle and minimum at 30°.
- Base steel show better performance than both the weld cases in all conditions in which erosion wear tests were performed.
- Weld with quench (weld bead with pure argon shielding gas) shows the lesser wear than the As weld (bead with argon shielding gas).
- Erosion wear rate is observed higher in initial running hours and reduces with respect to impingement angle as erosion causes strain hardening on the eroded surface due to which hardness of eroded surface also increases.
- The erosion of all the samples under normal impact are found that at 30° impingement angle the erosion loss is primarily due to shear cutting of surface material, whereas at 90° impingement angle resultant erosion damage is due to strain hardening and embrittlement of target material.
- Erosion wear increases with increase in erosion test time duration.

6.1 FUTURE SCOPE

- The erosion wear studies can be performed after welding the steel with different composition of shielding gases.
- Other parameters of erosion can be varied to study the effect on erosion.
- The computational approach can be used to simulate the similar work with different operating conditions.



REFERENCES

1. J.W. Simmons, "Overview: high-nitrogen alloying of stainless steels", *Materials Science and Engineering A*, 207 (1996), pp.159-169.
2. Rakesh Kumar, "Investigation Of Erosion Wear Of Ductile Materials With And Without Coating", M.Tech dissertation, Thapar university, July 2011.
3. Akhilesh K. Chauhan, D. B. Goel and Satya Prakash, "Erosion Behaviour of Hydro Turbine Steels", *Bull. Mater. Sci.*, Vol.31, No. 2, pp.115-120, 2008.
4. J.F. Santa, L.A. Espitia, J.A. Blanco, S.A. Romo, A. Toro "Slurry and cavitation erosion resistance of thermal spray coatings", *Wear* 267, pp.160-167, 2009.
5. R.C. Shivamurthy, M. Kamaraj, R. Nagarajan, S.M. Shariff, And G. Padmanabham, "Slurry Erosion Characteristics and Erosive Wear Mechanisms of Co- Based and Ni-Based Coatings Formed by Laser Surface Alloying", *The Minerals, Metals & Materials Society and ASM International*, volume 41a, 2010, pp.470- 486.
6. L. Finnie, "Erosion of Surfaces by Solid Particles", *Wear*, Vol. 3,1960, 87-103.
7. Levy, V. Alan, 1995, "Solid Particle Erosion and Erosion-Corrosion of Materials", *ASM International*, Materials Park, Ohio, (Chapter 8).
8. M.C. Lin, L.S. Chang, H.C. Lin, C.H. Yang, K.M. Lin "A study of high-speed slurry erosion of NiCrBSi thermal-sprayed coating" *Surface and Coating Technology*, 201, pp.3193-3198, 2006.
9. R. Mohammed, G. M. Reddy and K. S. Rao, 2017. Welding of nickel free high nitrogen stainless steel: Microstructure and mechanical properties. *Defence technology*, 13(2), pp.59-71.
10. O'Flynn, D. J., Bingley, M. S., Bradley, M. S. A., and Burnett, A. J., (2001), "A model to predict the solid particle erosion rate of metals and its assessment using heat-treated steels", *Wear*, 248, pp.162-177.
11. J. B. Zu, I. M. Ihtchings and G. T. Burstein "Design of a slurry erosion test rig", *Wear*, 140,

pp.331-344, 1990.

12. B. K. Prasad, Op Modi, A.K. Jha, A.K. Patwardhan “Effects of some material and experimental variables on the slurry wear characteristics of zinc aluminium alloy” ASM International, pp.75-80, 1999.
13. M. M. Stack, T.M. Abd El-Badia Some comments on mapping the combined effects of slurry concentration, impact velocity and electrochemical potential on the erosion-corrosion of WC/Co-Cr coatings, *Wear*, 264, pp.826-837, 2008.
14. Y. Iwai, T. Miyajima, A. Mizuno, T. Honda, T. Itou, S. Hogmark “Micro-Slurry-jet Erosion (MSE) testing of CVD TiC/TiN and TiC coatings”, *Wear*, 267, pp.264-269, 2009.
15. V. Borse Satish, B K Gandhi, “Nominal particle size of multi-sized particulate slurries for evaluation of erosion wear and effect of fine particles”, *Wear*, 257, 2004, pp.73-79.
16. T. Manisekaran, M. Kamaraj, S.M. Sharrif, and S.V. Joshi, “Slurry Erosion Studies on Surface Modified 13Cr-4Ni Steels: Effect of Angle of Impingement and Particle Size “, ASM International, (2006), pp.1059-9495.
17. S. Das, Y. S. Sarswati, D.P. Mondal, “Erosive Corrosive wear of aluminium alloy composites; influence of composition and speed”, *Wear*, 261(2006), pp.180 – 190.
18. Narendra M. Dube, Anirudh Dube, Deepak H. Veeregowda, Suman B. Iyer, “Experimental technique to analyse the slurry erosion wear due to turbulence”, *Wear* 267, pp.259-263, 2009.
19. G. R. Desale, B.K Gandhi, S.C Jain “Effect of erodent properties on erosion wear of ductile type materials”, *Wear*, 261, pp.914-921, 2006.
20. S. C. Mishra, S. Praharaj, Alok Satpathy, “Evaluation of erosion wear of a ceramic coating with Taguchi approach” *Journal of Manufacturing Engineering*, Vol.4, Issue.2, 2009.
21. A. Neville, F. Reza, S. Chiovelli, T. Revegab, “Erosion-corrosion behavior of WCbased MMCs in liquid-solid slurries”, *Wear*, pp.181-195, 2005.
22. O. P. Modi, Rupa Dasgupta, B.K. Prasad, A.K. Jha, A.H. Yegneswaran, and G. Dixit, “Erosion

of high carbon steel in coal and bottom- ash slurries”, Journal of Materials Engineering and performance, 2000, Volume 9(5).

23. Craig I. Walker, Greg C. Bodkin, “Empirical wear relationships for centrifugal slurry pumps Part 1: side-liners”, Wear, 242(2000), pp.140-146.

24. C. I. Walker, “Slurry pump side-liner wear: comparison of some laboratory and field results”, Wear, 250 (2001), pp.81-87.

25. S. N. Singh, B. K. Gandhi, “Study on the effect of surface orientation on erosion wear of flat specimens moving in a solid-liquid suspension”, Wear, 254(2003), pp.1233-1238.

26. H. Tian Harry, R. Addie Graeme, “Experimental study on erosive wear of some metallic materials using Coriolis wear testing approach”, Wear, 258 (2005), pp.458– 469.

27. C. N. Machio, G. Akdogan, M. J. Witcomb, S. Luyckx, “Performance of WC–VC–Co thermal spray coatings in abrasion and slurry erosion tests”, Wear, 258 (2005), pp.434–442.

28. Naveen Kumar, “Weldability aspects of Nitronic steel”, M.Tech dissertation, IIT Roorkee, May 2015.

